
Bridging the Gap Between Variational Inference and Wasserstein Gradient Flows

Mingxuan Yi, Song Liu
 School of Mathematics
 University of Bristol
 {mingxuan.yi, song.liu}@bristol.ac.uk

Abstract

Variational inference is a technique that approximates a target distribution by optimizing within the parameter space of variational families. On the other hand, Wasserstein gradient flows describe optimization within the space of probability measures where they do not necessarily admit a parametric density function. In this paper, we bridge the gap between these two methods. We demonstrate that, under certain conditions, the Bures-Wasserstein gradient flow can be recast as the Euclidean gradient flow where its forward Euler scheme is the standard black-box variational inference algorithm. Specifically, the vector field of the gradient flow is generated via the path-derivative gradient estimator. We also offer an alternative perspective on the path-derivative gradient, framing it as a distillation procedure to the Wasserstein gradient flow. Distillations can be extended to encompass f -divergences and non-Gaussian variational families. This extension yields a new gradient estimator for f -divergences, readily implementable using contemporary machine learning libraries like PyTorch or TensorFlow.

1 Introduction

An inference problem is generally difficult because it often requires dealing with a probability distribution only known up to a normalizing constant. Traditional statistical methods, such as Markov Chain Monte Carlo (MCMC), provide approximate solutions to such problems. However, MCMC struggles with high-dimensional challenges and is computationally intensive. An alternative is variational inference (Jordan et al., 1999; Blei et al., 2017), an optimization-based method to approximate the target probability distribution with a member (variational distribution) from a family of parametric models, denoted as $\{q(\mathbf{x}; \theta) | \theta \in \Theta\}$. Variational inference achieves these approximations by minimizing statistical divergences, which measure the disparity between the variational distribution $q(\mathbf{x}; \theta)$ and the target distribution $p(\mathbf{x})$. For example, a commonly used measurement is the (reverse) Kullback-Leibler (KL) divergence. Using this measurement, variational inference finds the best $q(\mathbf{x}; \hat{\theta})$ via,

$$\hat{\theta} = \operatorname{argmin}_{\theta \in \Theta} \operatorname{KL}(q_{\theta} || p) = \operatorname{argmin}_{\theta \in \Theta} \mathbb{E}_{\mathbf{x} \sim q_{\theta}} \left[\log \frac{q(\mathbf{x}; \theta)}{p(\mathbf{x})} \right]^1.$$

The advantage of variational inference is its adaptability. It can be applied to a wide range of models, from classical Bayesian models to more complex deep generative models. Furthermore, with the rise of deep learning libraries like TensorFlow (Abadi et al., 2016) and PyTorch (Paszke et al., 2019), variational inference can be easily implemented, scaled, and integrated with neural networks, making it a popular choice for modern machine learning tasks. Most VI techniques hinge

¹ q_{θ} represents $q(\mathbf{x}; \theta)$.

on deriving particular evidence bounds, facilitating the acquisition of a gradient estimator suitable for optimization.

Wasserstein gradient flows (Ambrosio et al., 2008) characterize a particle flow differential equation in the sample space where its associated marginal probability evolves with time to decrease a functional, e.g., the KL divergence as well. This differs from variational inference because the functional is decreased over the whole space of probability distributions where the distribution does not necessarily admit a parametric density function. A typical example is the Langevin stochastic differential equation (SDE),

$$d\mathbf{x}_t = \nabla_{\mathbf{x}} \log p(\mathbf{x}_t) dt + \sqrt{2} d\mathbf{w}_t, \quad (1)$$

where \mathbf{w}_t is the standard Wiener process, its marginals $\{q_t\}_{t \geq 0}$ can be viewed as the Wasserstein gradient flow of the KL divergence (Jordan et al., 1998; Otto, 2001). Wasserstein gradient flows have been widely studied in deep generative modelings (Ansari et al., 2021; Glaser et al., 2021; Yi et al., 2023) and sampling methods (Bernton, 2018; Cheng and Bartlett, 2018; Wibisono, 2018; Chewi et al., 2020). A previous work (Lambert et al., 2022) links Wasserstein gradient flows to variational inference by assuming the marginal probability admits a parametric Gaussian density function such that the continuous evolution of marginals and its discretization scheme can be obtained under the Bures-Wasserstein geometry.

Both variational inference and Wasserstein gradient flows optimize probability distributions by minimizing certain statistical discrepancies. However, they appear to operate in parallel rather than intersecting domains. In this paper, we bridge the gap between variational inference and Wasserstein gradient flows. Specifically, we unveil a surprising result that the Bures-Wasserstein gradient flow (Lambert et al., 2022) can be translated into a Euclidean gradient flow where its forward Euler scheme is exactly the black-box variational inference (BBVI) algorithm, with the Gaussian family but under different parameterizations. We show that the ordinary differential equation (ODE) system describing the Bures-Wasserstein gradient flow can be obtained via the path-derivative gradient estimator (Roeder et al., 2017). We further establish that the connection between the Euclidean gradient flow and the Bures-Wasserstein gradient flow arises from Riemannian submersion. In addition, we provide an alternative view on the path-derivative gradient as distillation which can be generalized to general f -divergences and non-Gaussian variational families. We obtain a novel gradient estimator for f -divergences which can be implemented by Pytorch or TensorFlow. We summarize our contributions as:

1. We bridge the gap between black-box variational inference and the Bures-Wasserstein gradient flows by showing the equivalence between them under certain conditions.
2. We provide an insight into the geometry on BBVI. This illustrates that the standard BBVI minimizing the KL divergence in the Euclidean geometry naturally involves the Wasserstein geometry.
3. We propose an alternative implementation of the path-derivative gradient estimator which can be generalized to f -divergences and non-Gaussian families.
4. A novel unbiased path-derivative gradient estimator of f -divergences is derived and this estimator generalizes previous works.

2 Background

In this section, we review preliminaries on variational inference and Wasserstein gradient flows. In this paper, all probability distributions are defined over the sample space \mathbb{R}^n , i.e., the standard Euclidean space.

2.1 Variational Inference

Variational inference (VI) reformulates inference problems as optimization problems. To allow for the optimization via the gradient descent algorithm, we need to compute the gradient of the KL divergence with respect to the parameter θ . If there exists a reparameterization $\mathbf{x}_\theta = g(\mathbf{z}; \theta) \sim q_\theta$, $\mathbf{z} \sim \xi$ where ξ is a base distribution and g transforms \mathbf{z} to \mathbf{x}_θ , we can obtain the gradient of the KL divergence as

$$\nabla_{\theta} \text{KL}(q_\theta || p) = \mathbb{E}_{\mathbf{z} \sim \xi} \left[\nabla_{\theta} \log \frac{q(\mathbf{x}_\theta; \theta)}{p(\mathbf{x}_\theta)} \right]. \quad (2)$$

The above Eq. (2) is called the reparameterization gradient estimator (Kingma and Welling, 2014; Rezende et al., 2014). The reparameterization gradient can be effortlessly implemented using auto-differentiation tools such as PyTorch (Paszke et al., 2019) and TensorFlow (Abadi et al., 2016), allowing us to bypass the need for model-specific derivations and enabling us to perform variational inference in a black-box manner (Ranganath et al., 2014), see Algorithm 1. An alternative is to use the score function gradient, details regarding the score function gradient can be found in (Mohamed et al., 2019).

Algorithm 1 Black-Box Variational Inference (Reparameterization gradient)

Require: target distribution $p(\mathbf{x})$, variational distribution $q(\mathbf{x}; \theta)$, learning rate τ .
while not converged **do**
 1. Sample $\mathbf{x}_\theta^i = g(\mathbf{z}^i; \theta) \sim q_\theta, \mathbf{z}^i \sim \xi$.
 2. Evaluate $L(\theta) = \frac{1}{N} \sum_i \log [q(\mathbf{x}_\theta^i; \theta)/p(\mathbf{x}_\theta^i)]$.
 3. $\theta \leftarrow \theta - \tau \nabla_\theta L(\theta)$ via back-propagation.
end while

However, the target distribution is sometimes only represented by an unnormalized density function $p(\mathbf{x})$. In order to evaluate the true density, we need to evaluate the normalizing constant $C = \int p(\mathbf{x})d\mathbf{x}$ such that $p_{\text{true}}(\mathbf{x}) = p(\mathbf{x})/C$, which is generally intractable. For example, to obtain the true density of the posterior distribution in Bayesian inference, the necessity arises to normalize the product of the likelihood and the prior, a task that frequently entails dealing with intractable integration. Variational inference mitigates this issue by leveraging the linearity of the logarithm function such that the normalizing constant does not affect the minimization of the KL divergence since

$$\text{KL}(q_\theta||p) = \text{KL}(q_\theta||p_{\text{true}}) + \log C.$$

$-\text{KL}(q_\theta||p)$ is called the evidence lower bound (ELBO) in the Bayesian inference setting (Blei et al., 2017).

2.2 Wasserstein Gradient Flows

Wasserstein gradient flows formulate the evolution of probability distributions over time by decreasing a functional on $\mathcal{P}(\mathbb{R}^n)$, where $\mathcal{P}(\mathbb{R}^n)$ refers to the space of probability distribution over \mathbb{R}^n with finite second moments. Let $(\mathcal{P}(\mathbb{R}^n), W_2)$ be a metric space of $\mathcal{P}(\mathbb{R}^n)$ equipped with Wasserstein-2 distance, and we denote this space as Wasserstein space. A curve $\{q_t\}_{t \geq 0} \in \mathcal{P}(\mathbb{R}^n)$ in the Wasserstein space is said to be the gradient flow of a functional $\mathcal{F}: \mathcal{P}(\mathbb{R}^n) \rightarrow \mathbb{R}$ if it satisfies the following continuity equation (Ambrosio et al., 2008),

$$\frac{\partial q_t}{\partial t} = \text{div}(q_t \nabla_{W_2} \mathcal{F}(q_t)). \quad (3)$$

$\nabla_{W_2} \mathcal{F}(q)$ is called the Wasserstein gradient of the functional $\mathcal{F}(q)$ which satisfies

$$\nabla_{W_2} \mathcal{F}(q) = \nabla_{\mathbf{x}} \frac{\delta \mathcal{F}(q)}{\delta q},$$

where $\nabla_{\mathbf{x}}$ is the Euclidean gradient operator and $\delta \mathcal{F}(q)/\delta q$ is the first variation of $\mathcal{F}(q)$. The Wasserstein gradient defines a family of vector fields $\{v_t\}_{t \geq 0}$ in Euclidean space \mathbb{R}^n which characterizes a probability flow ordinary differential equation (ODE),

$$d\mathbf{x}_t = v_t(\mathbf{x}_t)dt = -\nabla_{W_2} \mathcal{F}(q_t)(\mathbf{x}_t)dt. \quad (4)$$

This ODE describes the evolution of particle $\mathbf{x}_t \sim q_t$ in \mathbb{R}^n where the associated marginal q_t evolves to decrease $\mathcal{F}(q_t)$ along the direction of steepest descent according to the continuity equation in Eq. (3).

The Wasserstein gradient flow can be discretized via the following movement minimization scheme with step size τ , also known as the Jordan-Kinderlehrer-Otto (JKO) scheme² (Jordan et al., 1998),

$$q_{k+1}^\tau = \underset{q \in \mathcal{P}(\mathbb{R}^n)}{\text{argmin}} \left\{ \mathcal{F}(q) + \frac{1}{2\tau} W_2^2(q, q_k^\tau) \right\}, \quad (5)$$

² q_k^τ denotes the discretization of q_t with step size τ where k is the index of the discretized time.

the JKO scheme is to encourage q_{k+1}^τ to minimize the functional $\mathcal{F}(q)$ but stay close to q_k^τ in Wasserstein-2 distance as much as possible. It can be shown that as $\tau \rightarrow 0$, the limiting solution of Eq. (5) coincides with the curve $\{q_t\}_{t \geq 0}$ defined by the continuity equation in Eq. (3).

A special case of Wasserstein gradient flows is under the KL divergence $\mathcal{F}_{\text{kl}}(q) = \text{KL}(q||p)$, the continuity equation reads the Fokker-Planck equation

$$\frac{\partial q_t}{\partial t} = \text{div}(q_t(\nabla_{\mathbf{x}} \log q_t - \nabla_{\mathbf{x}} \log p)),$$

where the Wasserstein gradient is $\nabla_{W_2} \mathcal{F}_{\text{kl}}(q_t) = \nabla_{\mathbf{x}} \log(q_t/p)$ and the probability flow ODE follows

$$d\mathbf{x}_t = (\nabla_{\mathbf{x}} \log p(\mathbf{x}_t) - \nabla_{\mathbf{x}} \log q_t(\mathbf{x}_t)) dt. \quad (6)$$

The Fokker-Planck equation is also the continuity equation of the Langevin SDE in Eq. (1). The Langevin SDE and the probability flow ODE share the same marginals $\{q_t\}_{t \geq 0}$ if they evolve from the same initial q_0 .

3 Bures-Wasserstein Gradient Flows

In this section, we briefly review gradient flows defined in the Bures-Wasserstein space $(\mathcal{BW}(\mathbb{R}^n), W_2)$, i.e., the subspace of the Wasserstein space consisting of Gaussian distributions. We further show that black-box variational inference (BBVI) with the Gaussian family realizes the forward Euler scheme to the Bures-Wasserstein Gradient flows. Specifically, the vector fields of the ODE system describing the evolution of Gaussian mean and covariance (Lambert et al., 2022) can be obtained by the path-derivative (sticking the landing) gradient estimator (Roeder et al., 2017).

3.1 Bures-Wasserstein JKO Scheme

Recall that the Wasserstein-2 distance between two Gaussian distributions $q = \mathcal{N}(\mu, \Sigma)$ and $p = \mathcal{N}(\mu_p, \Sigma_p)$ has a closed form,

$$W_2^2(q, p) = \|\mu - \mu_p\|_2^2 + \mathcal{B}^2(\Sigma, \Sigma_p), \quad (7)$$

where $\mathcal{B}^2(\Sigma, \Sigma_p) = \text{tr}(\Sigma + \Sigma_p - 2(\Sigma^{\frac{1}{2}} \Sigma_p \Sigma^{\frac{1}{2}})^{\frac{1}{2}})$ is the squared Bures distance (Bures, 1969). By restricting the JKO scheme to the Bures-Wasserstein space,

$$q_{k+1}^\tau = \underset{q \in \mathcal{BW}(\mathbb{R}^n)}{\text{argmin}} \left\{ \text{KL}(q||p) + \frac{1}{2\tau} W_2^2(q, q_k^\tau) \right\},$$

Lambert et al. (2022) showed that the above discretization scheme yields a limiting curve $\{q_t : \mathcal{N}(\mu_t, \Sigma_t)\}_{t \geq 0}$ as a gradient flow of the KL divergence in the Bures-Wasserstein space where the means and covariance matrices of Gaussians follow an ODE system,

$$\begin{aligned} \frac{d\mu_t}{dt} &= \mathbb{E}_{\mathbf{x} \sim q_t} \left[\nabla_{\mathbf{x}} \log \frac{p(\mathbf{x})}{q_t(\mathbf{x})} \right], \\ \frac{d\Sigma_t}{dt} &= \mathbb{E}_{\mathbf{x} \sim q_t} \left[\left(\nabla_{\mathbf{x}} \log \frac{p(\mathbf{x})}{q_t(\mathbf{x})} \right)^T (\mathbf{x} - \mu_t) \right] + \mathbb{E}_{\mathbf{x} \sim q_t} \left[(\mathbf{x} - \mu_t)^T \nabla_{\mathbf{x}} \log \frac{p(\mathbf{x})}{q_t(\mathbf{x})} \right]. \end{aligned} \quad (8)$$

Notice that the Gaussian mean μ in this paper is the row vector, while some other literature uses the column vector formulation.

Remark 1. Eq. (8) the Hessian-free form of the covariance evolution, see Appendix A in (Lambert et al., 2022) or Appendix A in this paper for other equivalent forms of the ODE system, such as the Sarkka equation (Sarkka, 2007) in Bayesian filtering.

3.2 Unrolling Black-Box Variational Inference

In this section, we will show how black-box variational inference (BBVI) leads to the same ODE in Eq. (8). Performing BBVI with the standard gradient descent algorithm with the learning rate τ follows the iteration

$$\theta_{k+1}^\tau = \theta_k^\tau - \tau \nabla_{\theta} \text{KL}(q_{\theta}||p) \Big|_{\theta=\theta_k^\tau}. \quad (9)$$

We examine a particular kind of gradient estimator for the KL divergence as detailed below. Given the reparameterization $\mathbf{x}_\theta = g(\mathbf{z}; \theta) \sim q_\theta$, $\mathbf{z} \sim \xi$, the reparameterization gradient in Eq. (2) can be decomposed into two terms (Roeder et al., 2017),

$$\nabla_\theta \text{KL}(q_\theta || p) = \mathbb{E}_{\mathbf{z} \sim \xi} \left[\nabla_\theta \log \frac{q(\mathbf{x}_\theta; \theta)}{p(\mathbf{x}_\theta)} \right] = \underbrace{\mathbb{E}_{\mathbf{z} \sim \xi} \left[\nabla_{\mathbf{x}} \log \frac{q(\mathbf{x}_\theta; \theta)}{p(\mathbf{x}_\theta)} \circ \nabla_\theta \mathbf{x}_\theta \right]}_{\text{path-derivative gradient}} + \underbrace{\mathbb{E}_{\mathbf{x} \sim q_\theta} [\nabla_\theta \log q(\mathbf{x}; \theta)]}_{\text{score function}}. \quad (10)$$

Remark 2. The symbol "o" represents the application of the chain rule for each element in θ during backpropagation, e.g., if θ is a list (μ, S) , we apply the chain rule to μ and S individually. Such manipulation can be simply implemented via auto-differentiation libraries, we refer to (Paszke et al., 2019) and (Abadi et al., 2016) for more details.

The first term in Eq. (10) is called path-derivative gradient (Mohamed et al., 2019) since it requires differentiation through the reparameterized variable \mathbf{x}_θ which encodes the pathway from θ to the KL divergence. The second term cancels out because the score function has a zero mean. Roeder et al. (2017) proposed a simple efficient approach to implement this path-derivative gradient via a stop gradient operator, e.g., "detach" in PyTorch or "stop_gradient" in TensorFlow. We use the notation θ_s to denote the application of the stop gradient operator to the parameter θ . Once such an operator is applied, the differentiation through the variational parameter θ is discarded, i.e., θ_s can be regarded as a constant which is no longer trainable. Therefore, we can write the path-derivative gradient as

$$\nabla_\theta \text{KL}(q_\theta || p) = \mathbb{E}_{\mathbf{z} \sim \xi} \left[\nabla_\theta \log \frac{q(\mathbf{x}_\theta; \theta_s)}{p(\mathbf{x}_\theta)} \right]. \quad (11)$$

More details on the path-derivative gradient can be found in Appendix B.3.

Unlike the previous Section 3.1, we now consider the Gaussian variational family $\mathcal{N}(\mu, SS^T)$ with the parameter $\theta = (\mu, S)$ where S is the scale matrix, which avoids matrix decomposition to allow for the efficient reparameterization $\mathbf{x}_\theta = \mu + \mathbf{z}S^T \in \mathcal{N}(\mu, SS^T)$ with $\mathbf{z} \in \mathcal{N}(0, I)$. Proposition 1 provides a specific expression for the path derivative gradient given this Gaussian variational family.

Proposition 1 *If $q(\mathbf{x}; \theta) = \mathcal{N}(\mu, \Sigma)$ with $\Sigma = SS^T$ is a Gaussian distribution with parameter $\theta = (\mu, S)$ and the reparameterization is given by $\mathbf{x}_\theta = \mu + \mathbf{z}S^T$, $\mathbf{z} \sim \mathcal{N}(0, I)$. The path-derivative gradient in Eq. (10) or Eq. (11) is given by*

$$\begin{aligned} \nabla_\mu \text{KL}(q_\theta || p) &= -\mathbb{E}_{\mathbf{x} \sim q_\theta} \left[\nabla_{\mathbf{x}} \log \frac{p(\mathbf{x})}{q(\mathbf{x}; \theta)} \right], \\ \nabla_S \text{KL}(q_\theta || p) &= -\mathbb{E}_{\mathbf{x} \sim q_\theta} \left[\left(\nabla_{\mathbf{x}} \log \frac{p(\mathbf{x})}{q(\mathbf{x}; \theta)} \right)^T (\mathbf{x} - \mu) S^{-T} \right]. \end{aligned} \quad (12)$$

See the proof of Proposition 1 in Appendix B.4. By letting $\tau \rightarrow 0$, the gradient descent algorithm in Eq. (9) corresponds to an ODE system for $\theta_t = (\mu_t, S_t)$,

$$\begin{aligned} \frac{d\mu_t}{dt} &= \mathbb{E}_{\mathbf{x} \sim q_t} \left[\nabla_{\mathbf{x}} \log \frac{p(\mathbf{x})}{q_t(\mathbf{x})} \right], \\ \frac{dS_t}{dt} &= \mathbb{E}_{\mathbf{x} \sim q_t} \left[\left(\nabla_{\mathbf{x}} \log \frac{p(\mathbf{x})}{q_t(\mathbf{x})} \right)^T (\mathbf{x} - \mu_t) S_t^{-T} \right]. \end{aligned} \quad (13)$$

Using the fact $d\Sigma_t = (dS_t)S_t^T + S_t(dS_t^T)$, Eq. (13) implies the covariance evolution in Eq. (8). Note that the converse is not true because given a covariance matrix Σ , its decomposition $\Sigma = SS^T$ is not unique.

Proposition 1 suggests that the Bures-Wasserstein gradient flow can be equivalently derived through an alternative parameterization of Gaussians. Performing BBVI using the standard gradient descent (no momentum) is exactly the forward Euler scheme to the ODE in Eq. (13), although we still need to evaluate gradient estimators via Monte Carlo methods.

3.2.1 Geometry on Black-Box Variational Inference

The previous result is surprising because we have not introduced any specific geometry to BBVI but it leads to the same ODE system which is derived from the Bures-Wasserstein geometry. In this section, we advance our discussion by providing a comprehensive geometric analysis on BBVI.

Given $q_k^\tau = \mathcal{N}(\mu_k^\tau, S_k^\tau S_k^{\tau T})$, consider the following discretization scheme,

$$q_{k+1}^\tau = \operatorname{argmin}_{(\mu, S) \in \Theta} \left\{ \operatorname{KL}(q_\theta \| p) + \frac{1}{2\tau} (\|\mu - \mu_k^\tau\|_2^2 + \|S - S_k^\tau\|_F^2) \right\}, \quad (14)$$

where $\Theta : \mathbb{R}^n \times \mathbb{S}^{n \times n}$ is the parameter space and $\mathbb{S}^{n \times n}$ denotes the space of non-singular matrices. $\|A - B\|_F^2 = \operatorname{tr}(AA^T + BB^T - 2A^T B)$ is the squared Frobenius distance and its derivative is given by $\nabla_A \|A - B\|_F^2 = 2(A - B)$. Therefore, similar to the proximal method in Euclidean space, the discretization scheme in Eq. (14) leads to an implicit iteration for $\theta_k^\tau = (\mu_k^\tau, S_k^\tau)$,

$$\theta_{k+1}^\tau = \theta_k^\tau - \tau \nabla_\theta \operatorname{KL}(q_\theta \| p) \Big|_{\theta = \theta_{k+1}^\tau}.$$

which is the backward Euler scheme to the ODE in Eq. (13). It is obvious that the Frobenius distance between scales is equal to the Bures distance in Eq. (7) between covariances if the variational family is a mean-field Gaussian (diagonal covariance), but this is not true for the general case.

Similar to Takatsu (2011), next we only focus on the covariances of Gaussians by assuming they have zero means, since the difference between means in both Eq. (14) and Eq. (7) is just the Euclidean distance, which can be trivially generalized afterward. We consider two metric spaces as follows,

- $(\mathbb{S}^{n \times n}, F)$ is the space of non-singular matrices equipped with the Frobenius distance.
- $(\mathbb{C}^{n \times n}, \mathcal{B})$ is the space of positive-definite matrices equipped with the Bures distance.

Both $(\mathbb{S}^{n \times n}, F)$ and $(\mathbb{C}^{n \times n}, \mathcal{B})$ have Riemannian structures such that the associated Riemannian gradients can be defined. This section provides simplified main results on the Riemannian geometry, detailed discussions can be found in Appendix C.

Given a functional $\mathcal{F} : \mathbb{S}^{n \times n} \rightarrow \mathcal{R}$, the manifold on $\mathbb{S}^{n \times n}$ with the metric tensor \mathcal{G} by the Frobenius inner product $\langle A, B \rangle_{\mathcal{G}} = \operatorname{tr}(A^T B)$ has the Riemannian gradient as,

$$\operatorname{grad}_{\mathcal{G}} \mathcal{F}(S) = \nabla_S \mathcal{F}(S).$$

The Riemannian gradient is directly given by the matrix derivative $\nabla_S \mathcal{F}(S)$. This means optimization algorithms in the space $(\mathbb{S}^{n \times n}, F)$ are straightforward due to its "flat" geometry, akin to \mathbb{R}^n . Given this result, we call the ODE in Eq. (13) the Euclidean gradient flow of the KL divergence.

Remark 3. The term "Euclidean", while potentially a stretch from its strictest definition, might be slightly abused but is not misleading. The Frobenius inner product extends the concept of Euclidean inner product to the matrix space. Consequently, it inherits characteristics of flat geometry—like those associated with curvatures.

Next, we define a smooth map $\pi : \mathbb{S}^{n \times n} \rightarrow \mathbb{C}^{n \times n}$ as

$$\pi(S) = SS^T \in \mathbb{C}^{n \times n}.$$

The differential of this map $d\pi_S : \mathcal{T}_S \mathbb{S}^{n \times n} \rightarrow \mathcal{T}_{\pi(S)} \mathbb{C}^{n \times n}$ acts as

$$d\pi_S(X) = XS^T + SX^T, \quad X \in \mathcal{T}_S \mathbb{S}^{n \times n},$$

to map X from the tangent space at $S \in \mathbb{S}^{n \times n}$ to the tangent space at its image $\pi(S) \in \mathbb{C}^{n \times n}$. The differential map is obviously surjective such that the tangent space $\mathcal{T}_S \mathbb{S}^{n \times n}$ can be decomposed into two subspaces

$$\mathcal{T}_S \mathbb{S}^{n \times n} = \mathcal{V}_S \oplus \mathcal{H}_S,$$

where vertical space \mathcal{V}_S is the kernel of the differential map which comprises all elements that are mapped to zeros,

$$\mathcal{V}_S = \mathcal{K}d\pi_S = \{X | XS^T + SX^T = 0\},$$

and the horizontal space \mathcal{H}_S is the orthogonal complement to \mathcal{V}_S with respect to \mathcal{G} , given by

$$\mathcal{H}_S = \{X | XS^{-1} \text{ is symmetric}\}.$$

Geometrically, the kernel $\mathcal{K}d\pi_S$ represents the directions in which the mapping $\pi(S)$ is locally constant near the point $S \in \mathbb{S}^{n \times n}$. The decomposition determines that only horizontal vectors $X \in \mathcal{H}_S$ are mapped to $\mathcal{T}_{\pi(S)}\mathbb{C}^{n \times n}$.

Suppose that given a metric tensor \mathcal{Q} on $\mathbb{C}^{n \times n}$, [Takatsu \(2011\)](#) and [Bhatia et al. \(2019\)](#) showed that if the map π is a Riemannian submersion to satisfy

$$\langle d\pi_S(X), d\pi_S(Y) \rangle_{\mathcal{Q}} = \langle X, Y \rangle_{\mathcal{G}}, \quad \text{for } X, Y \in \mathcal{H}_S, \quad (15)$$

then the distance function induced by this metric tensor \mathcal{Q} is the Bures distance in Eq. (7). This suggests that we can translate the Bures-Wasserstein geometry into a more analytically tractable Euclidean geometry as discussed below.

Proposition 2 *The Euclidean gradient of the KL divergence with respect to the scale matrix S in Eq. (12) can be rewritten as*

$$\nabla_S \text{KL}(q_\theta || p) = -\mathbb{E}_{\mathbf{x} \sim q_\theta} [\nabla_{\mathbf{x}}^2 \log p(\mathbf{x})] \cdot S - S^{-T},$$

and it is horizontal, i.e., $\nabla_S \text{KL}(q_\theta || p) \in \mathcal{H}_S$.

Lemma 1 *Given two functionals: $\mathcal{F} : \mathbb{S}^{n \times n} \rightarrow \mathcal{R}$ and $\mathcal{E} : \mathbb{C}^{n \times n} \rightarrow \mathcal{R}$ satisfying*

$$\mathcal{F}(S) = \mathcal{E}(\pi(S)), \quad S \in \mathbb{S}^{n \times n}$$

where the map π is the Riemannian submersion satisfying Eq. (15). If $\text{grad}_{\mathcal{G}}\mathcal{F}(S)$ is horizontal, we have

$$\text{grad}_{\mathcal{Q}}\mathcal{E}(\pi(S)) = d\pi_S(\text{grad}_{\mathcal{G}}\mathcal{F}(S)).$$

Proofs for [Proposition 2](#) and [Lemma 1](#) can be found in [Appendix C.2](#) and [C.3](#) respectively. [Proposition 2](#) shows that the Euclidean gradient of the KL divergence with respect to the scale matrix has no vertical component such that it is exactly mapped to the tangent space $\mathcal{T}_{\pi(S)}\mathbb{C}^{n \times n}$ under the Riemannian submersion, to reconstruct the Riemannian gradient of the KL divergence with respect to the covariance matrix by [Lemma 1](#). The Riemannian gradient in $\mathbb{C}^{n \times n}$ is given by

$$\begin{aligned} \text{grad}_{\mathcal{Q}}\text{KL}(q_\theta || p) &= d\pi_S(\nabla_S \text{KL}(q_\theta || p)) \\ &= -2I - \mathbb{E}_{\mathbf{x} \sim q_\theta} [\nabla_{\mathbf{x}}^2 \log p(\mathbf{x})] \cdot \Sigma - \Sigma \cdot \mathbb{E}_{\mathbf{x} \sim q_\theta} [\nabla_{\mathbf{x}}^2 \log p(\mathbf{x})], \quad \Sigma = SS^T. \end{aligned}$$

This Riemannian gradient corresponds to the Hessian form (see Eq. (27)) of the ODE system in Eq. (8). As a result, the image of an Euclidean gradient flow in $(\mathbb{S}^{n \times n}, F)$ is also a gradient flow of the same functional in $(\mathbb{C}^{n \times n}, \mathcal{B})$. Furthermore, as a direct result of the Riemannian submersion, given a curve $\{\Sigma_t\}_{t \geq 0} \in \mathbb{C}^{n \times n}$, for any point $S_0 \in \pi^{-1}(\Sigma_0)$, the curve $\{S_t\}_{t \geq 0} \in \mathbb{S}^{n \times n}$ starting from S_0 with $\Sigma_t = S_t S_t^T$ is unique.

The above geometric analysis aligns with the previous result derived from the limiting case of the gradient descent algorithms. For a more in-depth discussion on Riemannian submersion, we direct the reader to [\(Petersen, 2006\)](#).

The horizontal space $\mathcal{H}_S = \{X | XS^{-1} \text{ is symmetric}\}$ indicates $\forall X \in \mathcal{H}_S, XS^{-1}$ is symmetric. In another coordinate system, we can also have $d\pi_S(X) = XS^{-1}$ (see [Proposition 3.1](#) by [Takatsu 2011](#)), this gives another form of Riemannian gradient in $\mathbb{C}^{n \times n}$ by [Lemma 1](#),

$$\begin{aligned} \text{grad}_{BW}\text{KL}(q_\theta || p) &= d\pi_S(\nabla_S \text{KL}(q_\theta || p)), \\ &= -\mathbb{E}_{\mathbf{x} \sim q_\theta} [\nabla_{\mathbf{x}}^2 \log p(\mathbf{x})] - \Sigma^{-1}, \quad \Sigma = SS^T, \end{aligned}$$

which is called the Bures-Wasserstein gradient studied by [Altschuler et al. \(2021\)](#); [Lambert et al. \(2022\)](#); [Diao et al. \(2023\)](#). Nevertheless, the geometry of the manifold is independent of the choice of coordinate system.

3.3 An Illustrative Example

In this part, we provide an illustrative example to see the empirical behaviors of three variational inference algorithms with the Gaussian family:

1. BBVI using the reparameterization gradient, see [Algorithm 1](#).
2. BBVI using the path-derivative gradient from Eq. (11).
3. The ODE in Eq. (8) by [Lambert et al. \(2022\)](#) where we use the forward Euler scheme (gradient descent).

The target distribution is a 2D Gaussian, and the initialization of the variational distribution remains the same across all three algorithms. We employ the Monte Carlo method to evaluate gradients, using the same sample size and learning rate for gradient descent in all cases. In addition, we also simulate the Langevin SDE in Eq. (1), which is commonly referred to as the Ornstein-Uhlenbeck (OU) process when the target distribution $p(\mathbf{x})$ is Gaussian. In this example, the marginals of the OU process remain Gaussian directly as a result of the Itô integral ([Wibisono, 2018](#)).

In [Figure 1](#), we can observe that three algorithms have the same evolutions as well as the OU process (ignoring the errors raised by Monte Carlo sampling and the discretization of gradient flows), especially, we can observe that BBVI with the path-derivative gradient and the ODE evolution both obey "sticking the landing" property (exact convergence without variance in terms of the trajectories and the Wasserstein-2 metrics) ([Roeder et al., 2017](#)). This is because the vector field (gradient) vanishes if the variational distribution closely approximates $p(\mathbf{x})$. More examples using larger sample sizes for Monte Carlo simulation and non-Gaussian target distributions are included in [Appendix E.1](#).

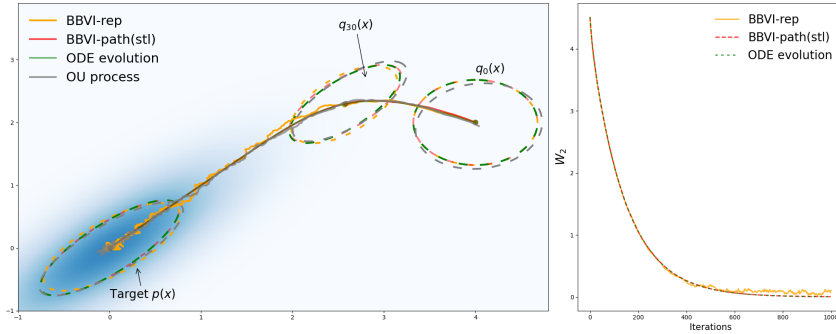


Figure 1: Trajectories of means of Gaussian variational distributions with variance ellipsoids at the initial, iteration 30 and the final step. The trajectory and variance ellipsoid for the OU process are evaluated empirically from particles. The right figure is the Wasserstein-2 distance between the variational and the target distributions. It can be seen that "BBVI-path(stl)" and "ODE evolution" have exact convergences without variances.

4 Distillation: An Alternative View Beyond the KL divergence and the Gaussian Family

We have established the relationship between BBVI and the Bures-Wasserstein gradient flow under the Gaussian variational family and the KL divergence. But how can we generalize it to f -divergences and non-Gaussian families? This section provides insights into this question. We first present an equivalent implementation of the path-derivative gradient using an iterative distillation procedure. We then extend this distillation to general f -divergences, leading to a novel gradient estimator. We demonstrate that this new estimator is statistically unbiased.

4.1 Distillation: From Sample Space to Parameter Space

We may have noticed that the path-derivative gradient in Eq. (10) generates the Wasserstein gradient of the KL divergence,

$$\nabla_{\theta} \text{KL}(q_{\theta} || p) = \mathbb{E}_{\mathbf{z} \sim \xi} [\nabla_{W_2} \mathcal{F}_{\text{kl}}(q_{\theta})(\mathbf{x}_{\theta}) \circ \nabla_{\theta} \mathbf{x}_{\theta}],$$

where $-\nabla_{W_2} \mathcal{F}_{\text{kl}}(q_\theta)(\mathbf{x}) = \nabla_{\mathbf{x}}(\log p(\mathbf{x})/q(\mathbf{x}; \theta))$ represents the vector field of the probability flow ODE of the KL divergence in Eq. (6). In this section, we will show that the path-derivative of the KL divergence can be equally implemented via an iterative distillation procedure, also known as the amortization trick (Wang and Liu, 2017; Yi et al., 2023).

First, suppose that at step k , q_k^τ represents the marginal distribution of the probability flow ODE in Eq. (6) with a parametric density function $q(\mathbf{x}; \theta)$ and v_k represents the vector field of the ODE, written as

$$v_k(\mathbf{x}) = \nabla_{\mathbf{x}}(\log p(\mathbf{x}) - \log q(\mathbf{x}; \theta)),$$

and particles are reparameterized by $\mathbf{x}_\theta = g(\mathbf{z}; \theta) \sim q_k^\tau$, $\mathbf{z} \sim \xi$. Next, we consider moving particles along the vector field with the step size τ , i.e., one-step forward Euler scheme,

$$\mathbf{x}' = \mathbf{x}_\theta + \tau v_k(\mathbf{x}_\theta).$$

In the space of probability distributions, this iteration corresponds to

$$q_{k+\frac{1}{2}}^\tau = [\text{id} - \tau \nabla_{W_2} \mathcal{F}_{\text{kl}}(q_\theta)]_{\#} q_k^\tau,$$

where $\#$ is the pushforward operator. The above forward proceeding operation is depicted in the following diagram,

$$\begin{array}{ccc} \text{Samples:} & \mathbf{x}_\theta & \xrightarrow{v_k} & \mathbf{x}' \\ & \downarrow & & \downarrow \\ \text{Marginals:} & q_k^\tau & \xrightarrow{-\nabla_{W_2} \mathcal{F}_{\text{kl}}(q_\theta)} & q_{k+\frac{1}{2}}^\tau \end{array}$$

Notice that $q_{k+\frac{1}{2}}^\tau$ has no closed-form density generally, and it is only represented by some particles \mathbf{x}' , see Figure 2.

The second step is to find a distribution $q_{k+1}^\tau = q(\mathbf{x}; \theta_{\text{new}})$ that numerically approximates $q_{k+\frac{1}{2}}^\tau$. Since the sample space is \mathbb{R}^n , a naive approach is to minimize the squared Euclidean distance between \mathbf{x}' and \mathbf{x}_θ via a single-step gradient descent,

$$\theta_{\text{new}} \leftarrow \theta_{\text{old}} - \nabla_{\theta} l(\theta)|_{\theta=\theta_{\text{old}}},$$

$$\text{where } l(\theta) = \frac{1}{2} \mathbb{E}_{\mathbf{z} \sim \xi} [\|\mathbf{x}_\theta - \mathbf{x}'\|_2^2],$$

where \mathbf{x}'_s means that the stop gradient operator is applied to \mathbf{x}' to discard the computational graph on θ , i.e., \mathbf{x}'_s becomes a fixed constant. Minimizing the loss function $l(\theta)$ encourages $g(\mathbf{z}; \theta)$ to draw particles as similar to \mathbf{x}' as possible. For example, in Figure 2, $g(\mathbf{z}; \theta)$ is encouraged to learn to draw the blue particles at $q_{k+\frac{1}{2}}^\tau$ which are closer to the target distribution. Applying ∇_{θ} to $l(\theta)$, we obtain

$$\nabla_{\theta} l(\theta) = \mathbb{E}_{\mathbf{z} \sim \xi} [(\mathbf{x}_\theta - \mathbf{x}'_s) \circ \nabla_{\theta} \mathbf{x}_\theta] = \tau \mathbb{E}_{\mathbf{z} \sim \xi} [\nabla_{W_2} \mathcal{F}_{\text{kl}}(q_\theta)(\mathbf{x}_\theta) \circ \nabla_{\theta} \mathbf{x}_\theta]. \quad (16)$$

This shows that $\nabla_{\theta} l(\theta)$ is equal to the path-derivative gradient of the KL divergence up to the step size τ , which means doing distillation is identical to performing BBVI with the path-derivative gradient. The difference here is that the stop gradient operator is applied to the updated particles \mathbf{x}' instead of the variational parameter θ . We summarize the distillation procedure as per iteration k :

1. sample particles \mathbf{x}_θ from $q_k^\tau = q(\mathbf{x}; \theta)$, and move particles via $\mathbf{x}' = \mathbf{x}_\theta + \tau v_k(\mathbf{x}_\theta)$.
2. apply the stop gradient operator to particles \mathbf{x}' and evaluate the loss $l(\theta)$.
3. backpropagate the loss $l(\theta)$ and update $\theta_{\text{new}} \leftarrow \theta_{\text{old}} - \nabla_{\theta} l(\theta)|_{\theta=\theta_{\text{old}}}$

The advantage of the distillation procedure is that it only relies on vector fields given by Wasserstein gradients and does not require explicit forms of the divergence and the variational family.

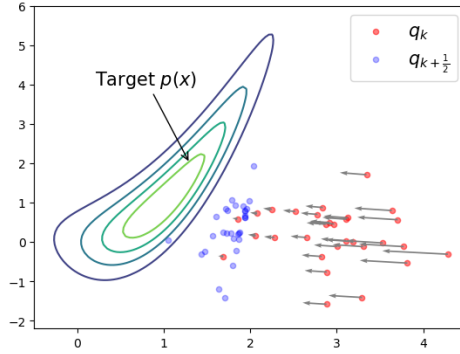


Figure 2: The target $p(\mathbf{x})$ is a banana distribution following the Rosenbrock density (Rosenbrock, 1960). If given q_k^τ as a Gaussian distribution, applying the Wasserstein gradient no longer guarantees particles from $q_{k+\frac{1}{2}}^\tau$ maintains Gaussian, see the blue particles.

4.2 Distilling the Probability Flow ODE of f -Divergence

In this section, we extend distillation to the probability flow ODE of f -divergence. The f -divergence is defined as

$$\mathcal{F}_f(q) = \mathcal{D}_f(p||q) = \int f\left(\frac{p(\mathbf{x})}{q(\mathbf{x})}\right) q(\mathbf{x}) d\mathbf{x},$$

where f is a convex function with $f(1) = 0$.

In order to apply the distillation procedure, we need to obtain the vector field for the probability flow ODE of f -divergence. Recall that in Eq. (4), the minus vector field is the Wasserstein gradient, which is given by the Euclidean gradient of the first variation. Lemma 2 offers an explicit expression of the first variation of f -divergences.

Lemma 2 *The first variation of $\mathcal{F}_f(q)$ is given by*

$$\frac{\delta \mathcal{F}_f(q)}{\delta q} = f(r) - r f'(r), \quad r = \frac{p}{q}.$$

The proof of Lemma 2 is provided in Appendix D.1 or alternatively, see Theorem 3.2 by Yi et al. (2023). By Lemma 2, the Wasserstein gradient of f -divergence is given by

$$\nabla_{W_2} \mathcal{F}_f(q) = \nabla_{\mathbf{x}} [f(r) - r f'(r)],$$

where the associated probability flow ODE is characterized by

$$d\mathbf{x}_t = \nabla_{\mathbf{x}} [r_t(\mathbf{x}) f'(r_t(\mathbf{x}_t)) - f(r_t(\mathbf{x}_t))] dt, \quad r_t = \frac{p}{q_t}. \quad (17)$$

Following the previous distillation procedure, if we move particles \mathbf{x}_θ along the vector field in Eq. (17) to \mathbf{x}' and evaluate the quadratic Euclidean distance $l(\theta)$ between them, we can obtain a novel gradient estimator by replacing $\nabla_{W_2} \mathcal{F}_{kl}(q)$ with $\nabla_{W_2} \mathcal{F}_f(q)$ in Eq. (16) such that

$$\nabla_{\theta} l(\theta) \propto \mathbb{E}_{\mathbf{z} \sim \xi} [\nabla_{W_2} \mathcal{F}_f(q_\theta)(\mathbf{x}_\theta) \circ \nabla_{\theta} \mathbf{x}_\theta]. \quad (18)$$

Similar to the path-derivative of the KL divergence (Roeder et al., 2017), Eq. (18) can be realized by applying the stop gradient operator to the parameter θ directly. By reorganizing Eq. (18), we obtain

$$\nabla_{\theta} l(\theta) \propto -\mathbb{E}_{\mathbf{z} \sim \xi} [\nabla_{\mathbf{x}} h(r(\mathbf{x}_\theta; \theta)) \circ \nabla_{\theta} \mathbf{x}_\theta] = -\mathbb{E}_{\mathbf{z} \sim \xi} [\nabla_{\theta} h(r(\mathbf{x}_\theta; \theta_s))] \quad (19)$$

where $h(r) = r f'(r) - f(r)$, and $r(\mathbf{x}; \theta_s) = p(\mathbf{x})/q(\mathbf{x}; \theta_s)$. It is obvious that Eq. (19) follows the straightforward result of the chain rule, or see Eq. (29) in Appendix B.3 for more discussions on the stop gradient operator.

4.2.1 Statistical Unbiasedness

The distillation procedure is simply based on heuristics. In this section, we show that the previously obtained estimator in Eq. (19) is an unbiased gradient estimator of f -divergence $\mathcal{D}_f(p||q_\theta)$ with respect to the parameter θ . We call this estimator the path-derivative gradient of f -divergence.

Proposition 3 *Given the reparameterization,*

$$\mathbf{x}_\theta = g(\mathbf{z}; \theta) \sim q(\mathbf{x}; \theta), \mathbf{z} \sim \xi,$$

the path-derivative gradient estimator of f -divergences is given by,

$$\nabla_{\theta} \mathcal{D}_f(p||q_\theta) = -\mathbb{E}_{\mathbf{z} \sim \xi} [\nabla_{\theta} h(r(\mathbf{x}_\theta; \theta_s))], \quad r(\mathbf{x}; \theta_s) = \frac{p(\mathbf{x})}{q(\mathbf{x}; \theta_s)}$$

where $h: \mathcal{R}^+ \rightarrow \mathcal{R}$ satisfies $h(r) = r f'(r) - f(r)$ and θ_s means the stop gradient operator is applied.

The proof of Proposition 3 can be found in Appendix D.2. It indicates that distilling the probability flow ODE of f -divergence is exactly equivalent to variational inference problems that use gradient descent to update parameters. Recall from Eq. (2) where we have the reparameterization gradient

of the KL divergence, similarly we can use this trick to obtain the reparameterization gradient of f -divergence (by using the law of unconscious statisticians and the interchange between differentiation and integration, see Appendix B) such that we have

$$\nabla_{\theta} \mathcal{D}_f(p||q_{\theta}) = \underbrace{\mathbb{E}_{\mathbf{z} \sim \xi} [\nabla_{\theta} f(r(\mathbf{x}_{\theta}; \theta))]}_{\text{reparameterization gradient}} = \underbrace{-\mathbb{E}_{\mathbf{z} \sim \xi} [\nabla_{\theta} h(r(\mathbf{x}_{\theta}; \theta_s))]}_{\text{path-derivative gradient}}.$$

The difference between these two estimators is that they are evaluated on entirely different Monte Carlo objectives. The reparameterization gradient requires a convex function f of the density ratio $r(\mathbf{x}; \theta) = p(\mathbf{x})/q(\mathbf{x}; \theta)$ that is differentiable with respect to both sample \mathbf{x} and parameter θ . The path-derivative gradient requires a non-decreasing function h of density ratio $r(\mathbf{x}; \theta_s)$ which is a function only differentiable with \mathbf{x} .

The path-derivative gradient also defines a surrogate loss function $L(\theta)$ which allows us to perform BBVI via

$$\min_{\theta} L(\theta) = -\mathbb{E}_{\mathbf{z} \sim \xi} [h(r(\mathbf{x}_{\theta}; \theta_s))], \quad \mathbf{x}_{\theta} = g(\mathbf{z}; \theta) \sim q(\mathbf{x}; \theta), \mathbf{z} \sim \xi \quad (20)$$

Remark 4. The convexity of f indicates that h is a non-decreasing function, due to that $h(r) = r f'(r) - f(r) \implies h'(r) = r f''(r) \geq 0$. If f is strictly convex which implies $f''(r) > 0$, the associated h is strictly increasing. In generative adversarial nets (GANs), Yi et al. (2023) showed that the generator loss of divergence GANs follows

$$-\mathbb{E}_{\mathbf{z} \sim \xi} [h(\hat{r}(\mathbf{x}_{\theta}))], \quad \mathbf{x}_{\theta} = g(\mathbf{z}; \theta) \sim p_{\text{generator}}, \quad (21)$$

where h can be an arbitrary increasing function and $\hat{r}(\mathbf{x})$ is the density ratio estimator of $p_{\text{data}}(\mathbf{x})/p_{\text{generator}}(\mathbf{x})$. The difference between Eq. (20) and Eq. (21) is that $\hat{r}(\mathbf{x})$ is obtained by two-sample density ratio estimation (Sugiyama et al., 2008; Moustakides and Basioti, 2019), and $r(\mathbf{x}; \theta_s)$ is obtained by applying the stop gradient operator to θ in the ground truth density ratio. It can be seen that both $r(\mathbf{x}; \theta_s)$ and $\hat{r}(\mathbf{x})$ are functions only with the variable \mathbf{x} .

4.2.2 Special Cases

The path-derivative gradient of f -divergence generalizes several gradient estimators.

- **(Reverse) KL divergence:** $f(r) = -\log r \implies h(r) = \log r - 1$,

$$-\mathbb{E}_{\mathbf{z} \sim \xi} [\nabla_{\theta} h(r(\mathbf{x}_{\theta}; \theta_s))] = \mathbb{E}_{\mathbf{z} \sim \xi} [\nabla_{\theta} \log [q(\mathbf{x}_{\theta}; \theta_s)/p(\mathbf{x}_{\theta})]], \quad (22)$$

we obtain the "sticking the landing" estimator (Roeder et al., 2017).

- **Forward KL divergence:** $f(r) = r \log r \implies h(r) = r$,

$$-\mathbb{E}_{\mathbf{z} \sim \xi} [\nabla_{\theta} h(r(\mathbf{x}_{\theta}; \theta_s))] = -\mathbb{E}_{\mathbf{z} \sim \xi} [\nabla_{\theta} [p(\mathbf{x}_{\theta})/q(\mathbf{x}_{\theta}; \theta_s)]] \quad (23)$$

this recovers the gradient estimator by Vaitl et al. (2022a).

- **α -divergence ($\alpha \neq 0$):** $f(r) = \frac{r^{\alpha} - \alpha r - (1-\alpha)}{\alpha(\alpha-1)} \implies h(r) = \frac{r^{\alpha} - 1}{\alpha}$,

$$-\mathbb{E}_{\mathbf{z} \sim \xi} [\nabla_{\theta} h(r(\mathbf{x}_{\theta}; \theta_s))] = -\mathbb{E}_{\mathbf{z} \sim \xi} \left[\frac{1}{\alpha} \nabla_{\theta} \left(\frac{p(\mathbf{x}_{\theta})}{q(\mathbf{x}_{\theta}; \theta_s)} \right)^{\alpha} \right], \quad (24)$$

this recovers the gradient estimator by Geffner and Domke (2021).

For an unnormalized density $p(\mathbf{x})$ where $p_{\text{true}}(\mathbf{x}) = p(\mathbf{x})/C$, we have

$$\left(\frac{p(\mathbf{x})}{q(\mathbf{x}; \theta_s)} \right)^{\alpha} \propto \left(\frac{p_{\text{true}}(\mathbf{x})}{q(\mathbf{x}; \theta_s)} \right)^{\alpha},$$

this shows that the normalizing constant only affects the scale of the gradient if the given divergence belongs to α -divergence family.

In Figure 3, we implement the path-derivative gradient for the Gaussian mixture variational family to approximate an unnormalized density function given by the Rosenbrock function (Rosenbrock, 1960) under different f -divergences. More empirical evaluations can be found in Appendix E.2, such as the comparison between the reparameterization and the path-derivative gradients, and Bayesian logistic regression on the UCI dataset (Asuncion and Newman, 2007).

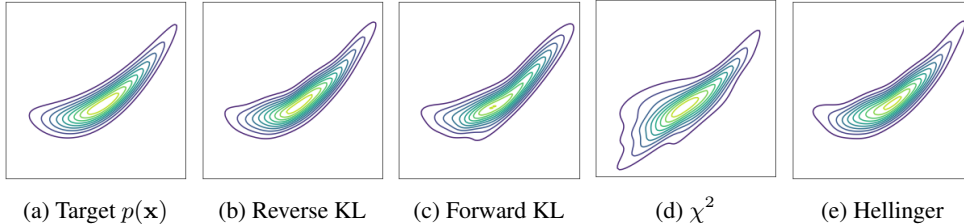


Figure 3: Contour plots of the target distribution, and the approximated Gaussian mixture models by minimizing various f -divergences (see Table 1 in Appendix D.2) using the path-derivative gradient.

5 Related Works

Bures-Wasserstein geometry. Lambert et al. (2022) first studied the variational inference problem under the Bures-Wasserstein geometry such that the mean and covariance evolution can be derived, subsequent work by Diao et al. (2023) investigated the forward-backward scheme to address the non-smoothness of the KL divergence. Together with another work by Altschuler et al. (2021) which studied the Bures-Wasserstein space for barycenter problems, all of these works consider parameterizing Gaussians with covariances such that the optimization algorithms are derived in a non-Euclidean space. The connection between the Euclidean space of non-singular matrices and the Bures space of positive-definite matrices was first established by Takatsu (2011); Modin (2016); Bhatia et al. (2019). Based on that, we showed that the gradient of the KL divergence w.r.t. the scale matrix of Gaussians is horizontal under the Riemannian submersion. This bypasses the difficulty in dealing with the non-Euclidean geometry and also demonstrates that conventional VI methods naturally involve the Wasserstein geometry.

Variational inference and path-derivative gradients. The standard variational inference methods consider the problem of minimizing the reverse KL divergence (Jordan et al., 1998; Kingma and Welling, 2014; Hoffman et al., 2013; Rezende et al., 2014; Blei et al., 2017). Minimizing the reverse KL divergence often results in mode-seeking tendencies and underestimates the uncertainties in the target distribution. To address this issue, other classes of f -divergence have also been studied, e.g., the forward KL divergence (Minka, 2013; Naesseth et al., 2020; Jerfel et al., 2021; Vaitl et al., 2022a), the α -divergence (Hernandez-Lobato et al., 2016; Li and Turner, 2016; Geffner and Domke, 2021). The majority of these VI methods are based on deriving specific evidence bounds to obtain a gradient estimator that allows for optimization whereas our gradient estimator is divergence-agnostic. We also noticed that our gradient estimator of f -divergence generalizes several works designing specific estimators using the stop gradient operator, e.g., the reverse KL divergence (Roeder et al., 2017), the forward KL divergence (Vaitl et al., 2022a), α -divergences (Geffner and Domke, 2021). To the best of our knowledge, the path-derivative gradient we introduced is the most unified form. The path-derivative gradient estimator relies on a stop-gradient operator, this operator also arises in importance-weighted variational objectives (Tucker et al., 2018; Finke and Thiery, 2019), doubly-reparameterized gradient (Bauer and Mnih, 2021), normalizing flow models (Agrawal et al., 2020; Vaitl et al., 2022b) and a low variance VI approach (Richter et al., 2020).

6 Discussion

In this paper, we bridge the gap between variational inference and Wasserstein gradient flows. Under certain conditions (Gaussian and the KL), we showed that the Bures-Wasserstein gradient flow can be obtained via the Euclidean gradient flow where its forward scheme is exactly the black-box variational inference algorithm. This equivalence is also a result of the Riemannian submersion which maps the Euclidean gradient to the Riemannian gradient in another space. We further showed that beyond the Gaussian family and the KL divergence, by distilling the Wasserstein gradient flows, we also obtained a new gradient estimator that is statistically unbiased. However, while the Gaussian variational family’s geometry is more straightforward, analyzing the geometry for a general parameter space remains to be challenging. Additionally, the variance analysis of the path-derivative gradient is still an unresolved matter.

References

- Martín Abadi, Ashish Agarwal, Paul Barham, Eugene Brevdo, Zhifeng Chen, Craig Citro, Greg S Corrado, Andy Davis, Jeffrey Dean, Matthieu Devin, et al. Tensorflow: Large-scale machine learning on heterogeneous distributed systems. *arXiv preprint arXiv:1603.04467*, 2016.
- Abhinav Agrawal, Daniel R Sheldon, and Justin Domke. Advances in black-box vi: Normalizing flows, importance weighting, and optimization. *In NeurIPS*, 2020.
- Jason Altschuler, Sinho Chewi, Patrik R Gerber, and Austin Stromme. Averaging on the bures-wasserstein manifold: dimension-free convergence of gradient descent. *Advances in Neural Information Processing Systems*, 34:22132–22145, 2021.
- Luigi Ambrosio, Nicola Gigli, and Giuseppe Savaré. *Gradient flows: in metric spaces and in the space of probability measures*. Springer Science & Business Media, 2008.
- Abdul Fatir Ansari, Ming Liang Ang, and Harold Soh. Refining deep generative models via discriminator gradient flow. *In ICLR*, 2021.
- Arthur Asuncion and David Newman. Uci machine learning repository, 2007.
- Matthias Bauer and Andriy Mnih. Generalized doubly reparameterized gradient estimators. *In ICML*, 2021.
- Espen Bernton. Langevin monte carlo and jko splitting. *In COLT*, 2018.
- Rajendra Bhatia, Tanvi Jain, and Yongdo Lim. On the bures–wasserstein distance between positive definite matrices. *Expositiones Mathematicae*, 37(2):165–191, 2019.
- David M Blei, Alp Kucukelbir, and Jon D McAuliffe. Variational inference: A review for statisticians. *Journal of the American statistical Association*, 112(518):859–877, 2017.
- Donald Bures. An extension of kakutani’s theorem on infinite product measures to the tensor product of semifinite w^* -algebras. *Transactions of the American Mathematical Society*, 135:199–212, 1969.
- Xiang Cheng and Peter Bartlett. Convergence of langevin mcmc in kl-divergence. *In ALT*, 2018.
- Sinho Chewi, Thibaut Le Gouic, Chen Lu, Tyler Maunu, and Philippe Rigollet. Svdg as a kernelized wasserstein gradient flow of the chi-squared divergence. *In NeurIPS*, 2020.
- Michael Ziyang Diao, Krishna Balasubramanian, Sinho Chewi, and Adil Salim. Forward-backward gaussian variational inference via jko in the bures-wasserstein space. *In International Conference on Machine Learning*, pages 7960–7991. PMLR, 2023.
- Adji Bousso Dieng, Dustin Tran, Rajesh Ranganath, John Paisley, and David Blei. Variational inference via χ upper bound minimization. *NeurIPS*, 2017.
- Axel Finke and Alexandre H Thiery. On importance-weighted autoencoders. *arXiv preprint arXiv:1907.10477*, 2019.
- Tomas Geffner and Justin Domke. On the difficulty of unbiased alpha divergence minimization. *In ICML*, 2021.
- Pierre Glaser, Michael Arbel, and Arthur Gretton. Kale flow: A relaxed kl gradient flow for probabilities with disjoint support. *NeurIPS*, 2021.
- Jose Hernandez-Lobato, Yingzhen Li, Mark Rowland, Thang Bui, Daniel Hernández-Lobato, and Richard Turner. Black-box alpha divergence minimization. *In ICML*, 2016.
- Matthew D Hoffman, David M Blei, Chong Wang, and John Paisley. Stochastic variational inference. *Journal of Machine Learning Research*, 2013.
- Aapo Hyvärinen and Peter Dayan. Estimation of non-normalized statistical models by score matching. *Journal of Machine Learning Research*, 6(4), 2005.

- Ghassen Jerfel, Serena Wang, Clara Wong-Fannjiang, Katherine A Heller, Yian Ma, and Michael I Jordan. Variational refinement for importance sampling using the forward kullback-leibler divergence. In *UAI*, 2021.
- Michael I Jordan, Zoubin Ghahramani, Tommi S Jaakkola, and Lawrence K Saul. An introduction to variational methods for graphical models. *Machine learning*, 37:183–233, 1999.
- Richard Jordan, David Kinderlehrer, and Felix Otto. The variational formulation of the fokker-planck equation. *SIAM journal on mathematical analysis*, 29(1):1–17, 1998.
- Diederik P Kingma and Max Welling. Auto-encoding variational bayes. In *ICLR*, 2014.
- Marc Lambert, Sinho Chewi, Francis Bach, Silvère Bonnabel, and Philippe Rigollet. Variational inference via wasserstein gradient flows. In *NeurIPS*, 2022.
- Yingzhen Li and Richard E Turner. Rényi divergence variational inference. *NeurIPS*, 2016.
- Thomas P Minka. Expectation propagation for approximate bayesian inference. *arXiv preprint arXiv:1301.2294*, 2013.
- Klas Modin. Geometry of matrix decompositions seen through optimal transport and information geometry. *arXiv preprint arXiv:1601.01875*, 2016.
- Shakir Mohamed, Mihaela Rosca, Michael Figurnov, and Andriy Mnih. Monte carlo gradient estimation in machine learning. arxiv e-prints, page. *arXiv preprint arXiv:1906.10652*, 2019.
- George V Moustakides and Kalliopi Basioti. Training neural networks for likelihood/density ratio estimation. *arXiv preprint arXiv:1911.00405*, 2019.
- Christian Naesseth, Fredrik Lindsten, and David Blei. Markovian score climbing: Variational inference with kl (pll q). *NeurIPS*, 2020.
- XuanLong Nguyen, Martin J Wainwright, and Michael I Jordan. Estimating divergence functionals and the likelihood ratio by convex risk minimization. *IEEE Transactions on Information Theory*, 56(11):5847–5861, 2010.
- Felix Otto. The geometry of dissipative evolution equations: the porous medium equation. *Communications in Partial Differential Equations*, 26:101–174, 2001.
- Adam Paszke, Sam Gross, Francisco Massa, Adam Lerer, James Bradbury, Gregory Chanan, Trevor Killeen, Zeming Lin, Natalia Gimelshein, Luca Antiga, et al. Pytorch: An imperative style, high-performance deep learning library. *Advances in neural information processing systems*, 32, 2019.
- Peter Petersen. *Riemannian geometry*, volume 171. Springer, 2006.
- Rajesh Ranganath, Sean Gerrish, and David Blei. Black box variational inference. In *Artificial intelligence and statistics*, pages 814–822. PMLR, 2014.
- Danilo Jimenez Rezende, Shakir Mohamed, and Daan Wierstra. Stochastic backpropagation and approximate inference in deep generative models. In *ICML*, 2014.
- Lorenz Richter, Ayman Boustati, Nikolas Nüsken, Francisco Ruiz, and Omer Deniz Akyildiz. Vargrad: a low-variance gradient estimator for variational inference. *NeurIPS*, 2020.
- Geoffrey Roeder, Yuhuai Wu, and David K Duvenaud. Sticking the landing: Simple, lower-variance gradient estimators for variational inference. In *NeurIPS*, 2017.
- HoHo Rosenbrock. An automatic method for finding the greatest or least value of a function. *The computer journal*, 3(3):175–184, 1960.
- Simo Sarkka. On unscented kalman filtering for state estimation of continuous-time nonlinear systems. *IEEE Transactions on automatic control*, 52(9):1631–1641, 2007.
- Yang Song, Jascha Sohl-Dickstein, Diederik P Kingma, Abhishek Kumar, Stefano Ermon, and Ben Poole. Score-based generative modeling through stochastic differential equations. In *ICLR*, 2021.

- Masashi Sugiyama, Taiji Suzuki, Shinichi Nakajima, Hisashi Kashima, Paul von Büna, and Motoaki Kawanabe. Direct importance estimation for covariate shift adaptation. *Annals of the Institute of Statistical Mathematics*, 60(4):699–746, 2008.
- Asuka Takatsu. Wasserstein geometry of gaussian measures. 2011.
- George Tucker, Dieterich Lawson, Shixiang Gu, and Chris J Maddison. Doubly reparameterized gradient estimators for monte carlo objectives. *arXiv preprint arXiv:1810.04152*, 2018.
- Lorenz Vaitl, Kim A Nicoli, Shinichi Nakajima, and Pan Kessel. Gradients should stay on path: better estimators of the reverse-and forward kl divergence for normalizing flows. *Machine Learning: Science and Technology*, 3(4):045006, 2022a.
- Lorenz Vaitl, Kim Andrea Nicoli, Shinichi Nakajima, and Pan Kessel. Path-gradient estimators for continuous normalizing flows. In *ICML, 2022b*.
- Pascal Vincent. A connection between score matching and denoising autoencoders. *Neural computation*, 23(7):1661–1674, 2011.
- Dilin Wang and Qiang Liu. Learning to draw samples: With application to amortized mle for generative adversarial learning. In *ICLR*, 2017.
- Andre Wibisono. Sampling as optimization in the space of measures: The langevin dynamics as a composite optimization problem. In *COLT*, 2018.
- Mingxuan Yi, Zhanxing Zhu, and Song Liu. Monoflow: Rethinking divergence gans via the perspective of wasserstein gradient flows. In *ICML*, 2023.

Appendix

Table of Contents

A	Equivalent Formulations of the ODE System	17
B	The Path-Derivative Gradient of the KL Divergence	18
B.1	Law of the Unconscious Statistician (LOTUS)	18
B.2	Interchange Between Differentiation and Integration	18
B.3	The Path-Derivative Gradient	18
B.4	Proof of Proposition 1	19
C	Riemannian Geometry	20
C.1	Preliminaries	20
C.2	Proof of Proposition 2	22
C.3	Proof of Lemma 1	22
C.4	Mapping A Curve Under Riemannian Submersion	23
D	The Path-Derivative Gradient of f-Divergence	24
D.1	Proof of Lemma 2	24
D.2	Proof of Proposition 3	24
E	Experiments	26
E.1	The Illustrative Example on Gaussians	26
E.2	On The Path-Derivative Gradient of f -Divergences	26
E.3	Bayesian Logistic Regression	27
E.4	Extension to Gaussian Mixture Models	28

A Equivalent Formulations of the ODE System

Given $q_t = \mathcal{N}(\mu_t, \Sigma_t)$, the ODE system following the Bures-Wasserstein gradient flow (Lambert et al., 2022) is given by

$$\begin{aligned}\frac{d\mu_t}{dt} &= \mathbb{E}_{\mathbf{x} \sim q_t} \left[\nabla_{\mathbf{x}} \log \frac{p(\mathbf{x})}{q_t(\mathbf{x})} \right], \\ \frac{d\Sigma_t}{dt} &= \mathbb{E}_{\mathbf{x} \sim q_t} \left[\left(\nabla_{\mathbf{x}} \log \frac{p(\mathbf{x})}{q_t(\mathbf{x})} \right)^T (\mathbf{x} - \mu_t) \right] + \mathbb{E}_{q_t} \left[(\mathbf{x} - \mu_t)^T \nabla_{\mathbf{x}} \log \frac{p(\mathbf{x})}{q_t(\mathbf{x})} \right].\end{aligned}$$

If the target distribution is an energy distribution $p(\mathbf{x}) = \exp[-V(\mathbf{x})]$, the mean evolution can be written as

$$\frac{d\mu_t}{dt} = \mathbb{E}_{\mathbf{x} \sim q_t} [\nabla_{\mathbf{x}} \log p(\mathbf{x})] = -\mathbb{E}_{\mathbf{x} \sim q_t} [\nabla_{\mathbf{x}} V(\mathbf{x})] \quad (25)$$

by the fact $\mathbb{E}_{\mathbf{x} \sim q_t} [\nabla_{\mathbf{x}} \log q_t(\mathbf{x})] = 0$ since q_t is a Gaussian.

Using $\mathbf{x} - \mu_t = -\nabla_{\mathbf{x}} \log q_t(\mathbf{x}) \cdot \Sigma_t$, the covariance evolution can be written as,

$$\begin{aligned}\frac{d\Sigma_t}{dt} &= \mathbb{E}_{\mathbf{x} \sim q_t} \left[\left(\nabla_{\mathbf{x}} \log \frac{p(\mathbf{x})}{q_t(\mathbf{x})} \right)^T (\mathbf{x} - \mu_t) \right] + \mathbb{E}_{q_t} \left[(\mathbf{x} - \mu_t)^T \nabla_{\mathbf{x}} \log \frac{p(\mathbf{x})}{q_t(\mathbf{x})} \right] \\ &= -\mathbb{E}_{\mathbf{x} \sim q_t} \left[\left(\nabla_{\mathbf{x}} \log \frac{p(\mathbf{x})}{q_t(\mathbf{x})} \right)^T \nabla_{\mathbf{x}} \log q_t(\mathbf{x}) \right] \cdot \Sigma_t - \Sigma_t^T \cdot \mathbb{E}_{q_t} \left[\nabla_{\mathbf{x}} \log q_t(\mathbf{x})^T \nabla_{\mathbf{x}} \log \frac{p(\mathbf{x})}{q_t(\mathbf{x})} \right].\end{aligned}$$

Using integral by part, we have

$$\mathbb{E}_{\mathbf{x} \sim q_t} \left[(\nabla_{\mathbf{x}} \log q_t(\mathbf{x}))^T \nabla_{\mathbf{x}} \log q_t(\mathbf{x}) \right] \cdot \Sigma_t = 0 - \mathbb{E}_{\mathbf{x} \sim q_t} [\nabla_{\mathbf{x}}^2 \log q_t(\mathbf{x})] \cdot \Sigma_t = I.$$

Hence the covariance evaluation can also be written as

$$\frac{d\Sigma_t}{dt} = 2I - \mathbb{E}_{\mathbf{x} \sim q_t} \left[(\nabla_{\mathbf{x}} V(\mathbf{x}))^T (\mathbf{x} - \mu_t) + (\mathbf{x} - \mu_t)^T \nabla_{\mathbf{x}} V(\mathbf{x}) \right], \quad (26)$$

Combing Eq. (25) and Eq. (26), we have

$$\begin{aligned}\frac{d\mu_t}{dt} &= -\mathbb{E}_{\mathbf{x} \sim q_t} [\nabla_{\mathbf{x}} V(\mathbf{x})] \\ \frac{d\Sigma_t}{dt} &= 2I - \mathbb{E}_{\mathbf{x} \sim q_t} \left[(\nabla_{\mathbf{x}} V(\mathbf{x}))^T (\mathbf{x} - \mu_t) + (\mathbf{x} - \mu_t)^T \nabla_{\mathbf{x}} V(\mathbf{x}) \right],\end{aligned}$$

this is known as the Sarkka equation in Bayesian filtering (Sarkka, 2007).

Using integral by part again, we obtain an equivalent Hessian form,

$$\begin{aligned}\frac{d\mu_t}{dt} &= -\mathbb{E}_{\mathbf{x} \sim q_t} [\nabla_{\mathbf{x}} V(\mathbf{x})] \\ \frac{d\Sigma_t}{dt} &= 2I - \Sigma_t \cdot \mathbb{E}_{\mathbf{x} \sim q_t} [\nabla_{\mathbf{x}}^2 V(\mathbf{x})] - \mathbb{E}_{\mathbf{x} \sim q_t} [\nabla_{\mathbf{x}}^2 V(\mathbf{x})] \cdot \Sigma_t\end{aligned} \quad (27)$$

B The Path-Derivative Gradient of the KL Divergence

In order to derive the path-derivative gradient (Roeder et al., 2017), we first present two preliminary results: the law of the unconscious statistician (LOTUS) and the interchange between differentiation and integration.

B.1 Law of the Unconscious Statistician (LOTUS)

LOTUS offers a straightforward method for computing the expectation under the change of variables. If there exists such a transformation (reparameterization),

$$\mathbf{x}_\theta = g(\mathbf{z}; \theta) \sim q(\mathbf{x}; \theta), \mathbf{z} \sim \xi.$$

By LOTUS, if given a function $\gamma: \mathbb{R}^n \rightarrow \mathbb{R}^m$, we have the following equality,

$$\mathbb{E}_{\mathbf{x} \sim q_\theta} [\gamma(\mathbf{x})] = \mathbb{E}_{\mathbf{z} \sim \xi} [\gamma(\mathbf{x}_\theta)] = \mathbb{E}_{\mathbf{z} \sim \xi} [\gamma(g(\mathbf{z}; \theta))].$$

B.2 Interchange Between Differentiation and Integration

Given $\mathbf{x} \in \mathcal{X}$, $\theta \in \Theta$ and a function $\psi: \mathcal{X} \times \Theta \rightarrow \mathcal{R}$. The availability of the interchange between differentiation and integration

$$\frac{\partial}{\partial \theta} \int \psi(\mathbf{x}; \theta) d\mathbf{x} = \int \frac{\partial}{\partial \theta} \psi(\mathbf{x}; \theta) d\mathbf{x},$$

holds if the following conditions are true,

- $\psi(\mathbf{x}; \theta)$ is differentiable with respect to θ , for almost all $\mathbf{x} \in \mathcal{X}$.
- $\psi(\mathbf{x}; \theta)$ is Lebesgue-integrable with respect to \mathbf{x} , for all $\theta \in \Theta$.
- There exists a Lebesgue-integrable function $g: \mathcal{X} \rightarrow \mathcal{R}$ such that all $\theta \in \Theta$ and almost all $\mathbf{x} \in \mathcal{X}$, the following inequality holds,

$$\left\| \frac{\partial}{\partial \theta} \psi(\mathbf{x}; \theta) \right\|_1 \leq g(\mathbf{x}).$$

These conditions are generally true in machine learning applications, we refer to (Mohamed et al., 2019) for more details.

B.3 The Path-Derivative Gradient

For a multivariate function $b(\mathbf{x}_\theta; \mathbf{y}_\theta): \mathcal{X} \times \mathcal{Y} \rightarrow \mathcal{R}$, its derivative with respect to θ is given by the chain rule,

$$\nabla_\theta b(\mathbf{x}_\theta; \mathbf{y}_\theta) = \nabla_{\mathbf{x}} b(\mathbf{x}_\theta; \mathbf{y}_\theta) \circ \nabla_\theta \mathbf{x}_\theta + \nabla_{\mathbf{y}} b(\mathbf{x}_\theta; \mathbf{y}_\theta) \circ \nabla_\theta \mathbf{y}_\theta.$$

Therefore, under the reparameterization $\mathbf{x}_\theta = g(\mathbf{z}; \theta)$, $\mathbf{z} \sim \xi$, we have

$$\begin{aligned} \nabla_\theta b(\mathbf{x}_\theta; \theta) &= \nabla_{\mathbf{x}} b(\mathbf{x}_\theta; \theta) \circ \nabla_\theta \mathbf{x}_\theta + \nabla_\theta b(\mathbf{x}; \theta)|_{\mathbf{x}=\mathbf{x}_\theta} \circ \nabla_\theta \theta \\ &= \nabla_{\mathbf{x}} b(\mathbf{x}_\theta; \theta) \circ \nabla_\theta \mathbf{x}_\theta + \nabla_\theta b(\mathbf{x}; \theta)|_{\mathbf{x}=\mathbf{x}_\theta}. \end{aligned} \quad (28)$$

In the second term $\nabla_\theta b(\mathbf{x}; \theta)|_{\mathbf{x}=\mathbf{x}_\theta}$, the differentiation operator ∇_θ works only with respect to the variational parameter θ .

If we apply the stop gradient operator to θ , this means the differentiation through the variational parameter θ is discarded such that we have

$$\nabla_\theta b(\mathbf{x}_\theta; \theta_s) = \nabla_{\mathbf{x}} b(\mathbf{x}_\theta; \theta) \circ \nabla_\theta \mathbf{x}_\theta \quad (29)$$

In terms of the algorithmic implementation, the stop gradient operator stops backpropagating losses into θ , this means θ_s becomes a non-trainable variable just like a constant.

Based on the above results, we now derive **the path-derivative gradient of the KL divergence** (Roeder et al., 2017).

Let $b(\mathbf{x}; \theta) = \log [q(\mathbf{x}; \theta)/p(\mathbf{x})]$ such that

$$\begin{aligned} \nabla_{\theta} \text{KL}(q_{\theta} || p) &= \mathbb{E}_{\mathbf{z} \sim \xi} [\nabla_{\theta} b(\mathbf{x}_{\theta}; \theta)] = \mathbb{E}_{\mathbf{z} \sim \xi} [\nabla_{\mathbf{x}} b(\mathbf{x}_{\theta}; \theta) \circ \nabla_{\theta} \mathbf{x}_{\theta} + \nabla_{\theta} b(\mathbf{x}; \theta)|_{\mathbf{x}=\mathbf{x}_{\theta}}] \\ &= \mathbb{E}_{\mathbf{z} \sim \xi} [\nabla_{\mathbf{x}} b(\mathbf{x}_{\theta}; \theta) \circ \nabla_{\theta} \mathbf{x}_{\theta}] + \mathbb{E}_{\mathbf{x} \sim q_{\theta}} [\nabla_{\theta} \log q(\mathbf{x}; \theta)], \text{ by LOTUS.} \\ &= \mathbb{E}_{\mathbf{z} \sim \xi} [\nabla_{\mathbf{x}} b(\mathbf{x}_{\theta}; \theta) \circ \nabla_{\theta} \mathbf{x}_{\theta}] + 0 \\ &= \mathbb{E}_{\mathbf{z} \sim \xi} [\nabla_{\theta} b(\mathbf{x}_{\theta}; \theta_s)] = \mathbb{E}_{\mathbf{z} \sim \xi} \left[\nabla_{\theta} \log \frac{q(\mathbf{x}_{\theta}; \theta_s)}{p(\mathbf{x}_{\theta})} \right] \end{aligned} \quad (30)$$

Remark: the score function $\nabla_{\theta} \log q(\mathbf{x}; \theta)$ has a zero mean by

$$\mathbb{E}_{\mathbf{x} \sim q_{\theta}} [\nabla_{\theta} \log q(\mathbf{x}; \theta)] = \int \nabla_{\theta} q(\mathbf{x}; \theta) d\mathbf{x} = \nabla_{\theta} \int q(\mathbf{x}; \theta) d\mathbf{x} = \nabla_{\theta}(1) = 0.$$

The score function here refers to the derivative of the log density with respect to the parameter θ , which is an enduring terminology in statistical inference. Alternatively, in the context of score matching methods (Hyvärinen and Dayan, 2005; Vincent, 2011), $\nabla_{\mathbf{x}} \log q(\mathbf{x}; \theta)$ is also referred to as the score function. The latter one is commonly used for score-based diffusion models (Song et al., 2021).

B.4 Proof of Proposition 1

If $q(\mathbf{x}; \theta) = \mathcal{N}(\mu, \Sigma)$ with $\Sigma = SS^T$ is a Gaussian distribution with the parameter $\theta = (\mu, S)$ and the reparameterization is given by $\mathbf{x}_{\theta} = \mu + \mathbf{z}S^T$, $\mathbf{z} \sim \mathcal{N}(0, I)$.

Specifications for dimensions:

$$\begin{aligned} \mathbf{x}, \mu, \mathbf{z} &: 1 \times n \text{ row vectors,} \\ S &: n \times n \text{ matrix.} \end{aligned}$$

The path-derivative gradient estimator (sticking the landing) (Roeder et al., 2017) of the KL divergence is

$$\nabla_{\theta} \text{KL}(q_{\theta} || p) = \mathbb{E}_{\mathbf{z} \sim \xi} \left[\nabla_{\mathbf{x}} \log \frac{q(\mathbf{x}_{\theta}; \theta_s)}{p(\mathbf{x}_{\theta})} \circ \nabla_{\theta} \mathbf{x}_{\theta} \right].$$

The gradient w.r.t. μ ,

The Jacobian $\nabla_{\mu} \mathbf{x}_{\theta}$ is

$$\nabla_{\mu} \mathbf{x}_{\theta} = I,$$

this is the standard Jacobian of vector-to-vector mappings. By the chain rule, the gradient w.r.t. μ is

$$\begin{aligned} \nabla_{\mu} \text{KL}(q_{\theta} || p) &= \mathbb{E}_{\mathbf{z} \sim \xi} \left[\nabla_{\mu} \log \frac{q(\mathbf{x}_{\theta}; \theta_s)}{p(\mathbf{x}_{\theta})} \right] = \mathbb{E}_{\mathbf{z} \sim \xi} \left[\nabla_{\mathbf{x}} \log \frac{q(\mathbf{x}_{\theta}; \theta_s)}{p(\mathbf{x}_{\theta})} \cdot I \right] \\ &= \mathbb{E}_{\mathbf{z} \sim \xi} \left[\nabla_{\mathbf{x}} \log \frac{q(\mathbf{x}_{\theta}; \theta)}{p(\mathbf{x}_{\theta})} \right] \\ &= -\mathbb{E}_{\mathbf{x} \sim q_{\theta}} \left[\nabla_{\mathbf{x}} \log \frac{p(\mathbf{x})}{q(\mathbf{x}; \theta)} \right], \text{ by LOTUS.} \end{aligned}$$

In the above equation, we can replace θ_s with θ since the operator $\nabla_{\mathbf{x}}$ is irrelevant to θ .

The gradient w.r.t. S ,

$\nabla_S \mathbf{x}_{\theta}$ is the Jacobian of matrix-to-vector mappings, its dimension is $(1 \times n) \times (n \times n)$, its element can be written

$$\begin{aligned} \frac{\partial \mathbf{x}_i}{\partial S_{i,k}} &= \mathbf{z}_k, \\ \frac{\partial \mathbf{x}_i}{\partial S_{j,k}} &= 0, \quad \text{if } i \neq j \end{aligned}$$

Similarly, the element-wise derivative w.r.t. the scale matrix is

$$\begin{aligned}\nabla_S \text{KL}(q_\theta || p)_{i,k} &= \mathbb{E}_{\mathbf{z} \sim \xi} \left[\nabla_S \log \frac{q(\mathbf{x}_\theta; \theta_s)}{p(\mathbf{x}_\theta)} \right]_{i,k} = \mathbb{E}_{\mathbf{z} \sim \xi} \left[\nabla_{\mathbf{x}_i} \log \frac{q(\mathbf{x}_\theta; \theta_s)}{p(\mathbf{x}_\theta)} \cdot \frac{\partial \mathbf{x}_i}{\partial S_{i,k}} \right] \\ &= \mathbb{E}_{\mathbf{z} \sim \xi} \left[\nabla_{\mathbf{x}_i} \log \frac{q(\mathbf{x}_\theta; \theta_s)}{p(\mathbf{x}_\theta)} \cdot \mathbf{z}_k \right].\end{aligned}$$

Hence, $\nabla_S \text{KL}(q_\theta || p)_{i,k}$ is the mean of the product of the i -th element of $\nabla_{\mathbf{x}} \log \frac{q(\mathbf{x}_\theta; \theta)}{p(\mathbf{x}_\theta)}$ and the k -th element of \mathbf{z} . We can write $\nabla_S \text{KL}(q_\theta || p)$ as

$$\begin{aligned}\nabla_S \text{KL}(q_\theta || p) &= \mathbb{E}_{\mathbf{z} \sim \xi} \left[\left(\nabla_{\mathbf{x}} \log \frac{q(\mathbf{x}_\theta; \theta)}{p(\mathbf{x}_\theta)} \right)^T \cdot \mathbf{z} \right] \\ &= \mathbb{E}_{\mathbf{z} \sim \xi} \left[\left(\nabla_{\mathbf{x}} \log \frac{q(\mathbf{x}_\theta; \theta)}{p(\mathbf{x}_\theta)} \right)^T \cdot (\mathbf{x}_\theta - \mu) S^{-T} \right], \quad \mathbf{z} = (\mathbf{x}_\theta - \mu) S^{-T} \\ &= -\mathbb{E}_{\mathbf{x} \sim q_\theta} \left[\left(\nabla_{\mathbf{x}} \log \frac{p(\mathbf{x})}{q(\mathbf{x}; \theta)} \right)^T (\mathbf{x} - \mu) S^{-T} \right], \text{ by LOTUS.}\end{aligned}$$

C Riemannian Geometry

C.1 Preliminaries

1. The space of non-singular matrices:

The space of $\mathbb{S}^{n \times n}$ can be endowed with the Riemannian structure given a metric tensor \mathcal{G} induced by the Frobenius inner product. That is, for a point $S \in \mathbb{S}^{n \times n}$, we denote its tangent space as $\mathcal{T}_S \mathbb{S}^{n \times n}$, then for $A, B \in \mathcal{T}_S \mathbb{S}^{n \times n}$, metric tensor \mathcal{G} is given by

$$\langle A, B \rangle_{\mathcal{G}} = \text{tr}(A^T B).$$

Given a (smooth) functional $\mathcal{F} : \mathbb{S}^{n \times n} \rightarrow \mathcal{R}$, the Riemannian gradient $\text{grad}_{\mathcal{G}} \mathcal{F}(S) \in \mathcal{T}_S \mathbb{S}^{n \times n}$ is defined as,

$$\forall X \in \mathcal{T}_S \mathbb{S}^{n \times n}, \quad \langle \text{grad}_{\mathcal{G}} \mathcal{F}(S), X \rangle_{\mathcal{G}} = d\mathcal{F}_S(X), \quad (31)$$

where $d\mathcal{F}_S(X)$ is the differential of \mathcal{F} given by

$$d\mathcal{F}_S(X) = \lim_{t \rightarrow 0} \frac{\mathcal{F}(S + tX) - \mathcal{F}(S)}{t} = \text{tr}(\nabla_S \mathcal{F}(S)^T X).$$

Therefore,

$$\langle \text{grad}_{\mathcal{G}} \mathcal{F}(S), X \rangle_{\mathcal{G}} = \text{tr}(\nabla_S \mathcal{F}(S)^T X) \implies \text{grad}_{\mathcal{G}} \mathcal{F}(S) = \nabla_S \mathcal{F}(S),$$

the Riemannian gradient on the manifold $(\mathbb{S}^{n \times n}, \mathcal{G})$ is the matrix derivative itself (Euclidean gradient).

It is intuitive to think of the manifold $(\mathbb{S}^{n \times n}, \mathcal{G})$ as being analogous to the Euclidean space \mathbb{R}^n of vectors since \mathcal{G} is a flat metric tensor.

2. Riemannian submersion:

Let $(\mathbb{C}^{n \times n}, \mathcal{Q})$ be another manifold with the metric tensor \mathcal{Q} and π be a smooth map $\pi : \mathbb{S}^{n \times n} \rightarrow \mathbb{C}^{n \times n}$. If the differential map $d\pi_S : \mathcal{T}_S \mathbb{S}^{n \times n} \rightarrow \mathcal{T}_{\pi(S)} \mathbb{C}^{n \times n}$ is surjective, the tangent space $\mathcal{T}_S \mathbb{S}^{n \times n}$ can be decomposed into a vertical space \mathcal{V}_S and a horizontal space \mathcal{H}_S ,

$$\mathcal{T}_S \mathbb{S}^{n \times n} = \mathcal{V}_S \oplus \mathcal{H}_S.$$

The vertical space is the kernel of the differential map which comprises all elements that are mapped to zeros,

$$\mathcal{V}_S = \mathcal{K}d\pi_S = \{X | d\pi_S(X) = 0\},$$

and the horizontal space is its orthogonal complement with respect to the metric tensor \mathcal{G} ,

$$\forall Y \in \mathcal{H}_S \text{ and } \forall X \in \mathcal{V}_S, \quad \langle Y, X \rangle_{\mathcal{G}} = 0.$$

Geometrically, the kernel $\mathcal{K}d\pi_S$ represents the directions in which the mapping $\pi(S)$ is locally constant near the point $S \in \mathbb{S}^{n \times n}$.

We say the map $\pi : \mathbb{S}^{n \times n} \rightarrow \mathbb{C}^{n \times n}$ is a **Riemannian submersion** if and only if for $S \in \mathbb{S}^{n \times n}$, the differential map $d\pi_S$ is surjective and it maps the horizontal space \mathcal{H}_S to $\mathcal{T}_{\pi(S)}\mathbb{C}^{n \times n}$ isometrically, i.e.,

$$\langle d\pi_S(X), d\pi_S(Y) \rangle_{\mathcal{Q}} = \langle X, Y \rangle_{\mathcal{G}}, \quad X, Y \in \mathcal{H}_S.$$

3. Properties of $\pi(S) = SS^T$:

The differential of the map is given by $d\pi_S(X) = XS^T + SX^T$, $X \in \mathcal{T}_S\mathbb{S}^{n \times n}$.

By the definition, the vertical space \mathcal{V}_S is given by the kernel $\mathcal{K}d\pi_S = \{X | XS^T + SX^T = 0\}$.

To find the horizontal space \mathcal{H}_S , let $X \in \mathcal{V}_S$ which indicates XS^T is skew-symmetric, $\forall Y \in \mathcal{H}_S$, Y is orthogonal to X by

$$\begin{aligned} \langle Y, X \rangle_{\mathcal{G}} &= \text{tr}(Y^T X) = 0 \\ \implies \text{tr}(Y^T X S^T S^{-T}) &= 0 \implies \text{tr}(S^{-T} Y^T X S^T) = 0 \iff Y S^{-1} \text{ is symmetric.} \end{aligned}$$

This gives the horizontal space $\mathcal{H}_S = \{Y | Y S^{-1} \text{ is symmetric}\}$. Note that for $Z \in \mathcal{T}_S\mathbb{S}^{n \times n}$, only its horizontal component is mapped to $\mathcal{T}_{\pi(S)}\mathbb{C}^{n \times n}$ because the vertical component is mapped to zero.

4. The space of positive-definite matrices:

By Theorem 3 and Theorem 5 by (Bhatia et al., 2019), for $\pi(S) = SS^T$ to qualify as a Riemannian submersion, there exists a unique metric tensor \mathcal{Q} on $\mathbb{C}^{n \times n}$, for $A = \pi(S) = SS^T \in \mathbb{C}^{n \times n}$, and $Y, Z \in \mathcal{T}_A\mathbb{C}^{n \times n}$ given by the differential of the map $Y = d\pi_S(HS) = HA + AH$ and $Z = d\pi_S(KS) = KA + AK$, where H and K are symmetric matrices to ensure HS and KS lie within the horizontal space, the inner product of \mathcal{Q} must be given by

$$\langle Y, Z \rangle_{\mathcal{Q}} = \langle HA + AH, KA + AK \rangle_{\mathcal{Q}} = \langle HS, KS \rangle_{\mathcal{G}} = \text{tr}(KAH)$$

such that the induced distance function by this metric tensor \mathcal{Q} is the Bures distance \mathcal{B} ,

$$\forall A, B \in \mathbb{C}^{n \times n}, \quad \mathcal{B}^2(A, B) = \|A^{\frac{1}{2}} - B^{\frac{1}{2}}U\|_F^2 = \text{tr}(A + B - 2(A^{\frac{1}{2}}BA^{\frac{1}{2}})^{\frac{1}{2}}),$$

where $U = B^{\frac{1}{2}}A^{\frac{1}{2}}(A^{\frac{1}{2}}BA^{\frac{1}{2}})^{-\frac{1}{2}}$ is a unitary matrix by the polar decomposition of $A^{\frac{1}{2}}B^{\frac{1}{2}}$. $B^{\frac{1}{2}}U$ can be written as

$$B^{\frac{1}{2}}U = T_{A \rightarrow B}A^{\frac{1}{2}}, \quad T_{A \rightarrow B} = A^{-\frac{1}{2}}(A^{\frac{1}{2}}BA^{\frac{1}{2}})^{\frac{1}{2}}A^{-\frac{1}{2}},$$

where $T_{A \rightarrow B} : \mathbb{R}^n \rightarrow \mathbb{R}^n$ is the optimal transport map of moving mass from $\mathcal{N}(0, A)$ to $\mathcal{N}(0, B)$.

The geodesic connecting $A, B \in \mathbb{C}^{n \times n}$ under the metric tensor \mathcal{Q} is

$$\Sigma_t = ((1-t)I + tT_{A \rightarrow B})A((1-t)I + tT_{A \rightarrow B}), \quad t \in [0, 1],$$

where $\Sigma_0 = A$ and $\Sigma_1 = B$.

The Bures distance can be expressed by the length of another geodesic on $\mathbb{S}^{n \times n}$ connecting $A^{\frac{1}{2}}, B^{\frac{1}{2}}U \in \mathbb{S}^{n \times n}$ under the metric tensor \mathcal{G} ,

$$S_t = ((1-t)I + tT_{A \rightarrow B})A^{\frac{1}{2}}, \quad t \in [0, 1],$$

where $S_0 = A^{\frac{1}{2}}$ and $S_1 = B^{\frac{1}{2}}U$.

C.2 Proof of Proposition 2

Here we assume $q = \mathcal{N}(0, \Sigma)$ where the covariance matrix is $\Sigma = SS^T$, and the gradient of the KL divergence w.r.t. S is given by the Proposition 1,

$$\nabla_S \text{KL}(q_\theta || p) = -\mathbb{E}_{\mathbf{x} \sim q_\theta} \left[\left(\nabla_{\mathbf{x}} \log \frac{p(\mathbf{x})}{q(\mathbf{x}; \theta)} \right)^T \mathbf{x} S^{-T} \right].$$

Using $\log q(\mathbf{x}; \theta) = -\mathbf{x} S^{-T} S^{-1} \mathbf{x}^T$, $\nabla_{\mathbf{x}} \log q(\mathbf{x}; \theta) = -\mathbf{x} S^{-T} S^{-1}$ and $\nabla_{\mathbf{x}}^2 \log q(\mathbf{x}; \theta) = -S^{-T} S^{-1}$, we rewrite

$$\begin{aligned} -\mathbb{E}_{\mathbf{x} \sim q_\theta} \left[\left(\nabla_{\mathbf{x}} \log \frac{p(\mathbf{x})}{q(\mathbf{x}; \theta)} \right)^T \mathbf{x} S^{-T} \right] &= \mathbb{E}_{\mathbf{x} \sim q_\theta} \left[\left(\nabla_{\mathbf{x}} \log \frac{p(\mathbf{x})}{q(\mathbf{x}; \theta)} \right)^T \nabla_{\mathbf{x}} \log q(\mathbf{x}; \theta) \right] \cdot S \\ &= \left[\int \left(\nabla_{\mathbf{x}} \log \frac{p(\mathbf{x})}{q(\mathbf{x}; \theta)} \right)^T \nabla_{\mathbf{x}} q(\mathbf{x}; \theta) d\mathbf{x} \right] \cdot S \\ &= - \left[\int \nabla_{\mathbf{x}}^2 \log \frac{p(\mathbf{x})}{q(\mathbf{x}; \theta)} q(\mathbf{x}; \theta) d\mathbf{x} \right] \cdot S \\ &= -\mathbb{E}_{\mathbf{x} \sim q_\theta} \left[\nabla_{\mathbf{x}}^2 \log p(\mathbf{x}) - \nabla_{\mathbf{x}}^2 \log q(\mathbf{x}; \theta) \right] \cdot S \\ &= -\mathbb{E}_{\mathbf{x} \sim q_\theta} \left[\nabla_{\mathbf{x}}^2 \log p(\mathbf{x}) \right] \cdot S - S^{-T} \end{aligned}$$

$\mathbb{E}_{\mathbf{x} \sim q_\theta} \left[\nabla_{\mathbf{x}}^2 \log p(\mathbf{x}) \right]$ is the expectation of the Hessian matrix, hence it is symmetric, let it be A such that we write the gradient of the KL divergence as

$$\nabla_S \text{KL}(q_\theta || p) = -AS - S^{-T}.$$

The horizontal space is expressed by

$$\mathcal{H}_S = \{X | XS^{-1} \text{ is symmetric}\}.$$

Let $H = -A - S^{-T} S^{-1}$ such that $\nabla_S \text{KL}(q_\theta || p) = -AS - S^{-T} = HS$. A and $S^{-T} S^{-1}$ are symmetric matrices, hence H is symmetric $\implies \nabla_S \text{KL}(q_\theta || p) \in \mathcal{H}_S$.

C.3 Proof of Lemma 1

Given two functionals: $\mathcal{F} : \mathbb{S}^{n \times n} \rightarrow \mathcal{R}$ and $\mathcal{E} : \mathbb{C}^{n \times n} \rightarrow \mathcal{R}$ satisfying

$$\mathcal{F}(S) = \mathcal{E}(\pi(S)).$$

For $X \in \mathcal{T}_S \mathbb{S}^{n \times n}$, we have the differential $d\mathcal{F}_S(X) = d\mathcal{E}_{\pi(S)}(d\pi_S(X))$ by chain rule. Now, Eq. (31) rewrites as

$$\forall X \in \mathcal{T}_S \mathbb{S}^{n \times n}, \quad \langle \text{grad}_{\mathcal{G}} \mathcal{F}(S), X \rangle_{\mathcal{G}} = d\mathcal{E}_{\pi(S)}(d\pi_S(X)), \quad (32)$$

By the assumption $\text{grad}_{\mathcal{G}} \mathcal{F}(S)$ is horizontal, so that $\text{grad}_{\mathcal{G}} \mathcal{F}(S)$ is orthogonal to the vertical component of X . Hence, we have

$$\langle \text{grad}_{\mathcal{G}} \mathcal{F}(S), X \rangle_{\mathcal{G}} = \langle \text{grad}_{\mathcal{G}} \mathcal{F}(S), X_{\mathcal{H}} \rangle_{\mathcal{G}},$$

where $X_{\mathcal{H}}$ represents the horizontal component of X .

Since π is a Riemannian submersion which gives $\langle d\pi_S(X), d\pi_S(Y) \rangle_{\mathcal{Q}} = \langle X, Y \rangle_{\mathcal{G}}$, $X, Y \in \mathcal{H}_S$, thus we have

$$\langle d\pi_S(\text{grad}_{\mathcal{G}} \mathcal{F}(S)), d\pi_S(X) \rangle_{\mathcal{Q}} = \langle \text{grad}_{\mathcal{G}} \mathcal{F}(S), X_{\mathcal{H}} \rangle_{\mathcal{G}} = d\mathcal{E}_{\pi(S)}(d\pi_S(X))$$

By the definition of the Riemannian gradient

$$\forall Y \in \mathcal{T}_{\pi(S)} \mathbb{C}^{n \times n}, \quad \langle \text{grad}_{\mathcal{Q}} \mathcal{E}(\pi(S)), Y \rangle_{\mathcal{Q}} = d\mathcal{E}_{\pi(S)}(Y),$$

the Riemannian gradient on $\mathbb{C}^{n \times n}$ with the metric tensor \mathcal{Q} must be given by

$$\text{grad}_{\mathcal{Q}} \mathcal{E}(\pi(S)) = d\pi_S(\text{grad}_{\mathcal{G}} \mathcal{F}(S)).$$

C.4 Mapping A Curve Under Riemannian Submersion

Under the Riemannian submersion, a curve $\{S_t\}_{t \geq 0}$ in $\mathbb{S}^{n \times n}$ is a horizontal lift if it satisfies

$$\frac{dS_t}{dt} = H(t)S_t, \quad (33)$$

if $H(t)$ is a symmetric matrix. Obviously from [Proposition 2](#), the Euclidean gradient flow $\{S_t\}_{t \geq 0}$ is horizontal with the symmetric matrix

$$H(t) = \mathbb{E}_{\mathbf{x} \sim q_t} [\nabla_{\mathbf{x}}^2 \log p(\mathbf{x})] + S_t^{-T} S_t^{-1}. \quad (34)$$

The corresponding curve in $\mathbb{C}^{n \times n}$ is

$$\begin{aligned} \frac{d\Sigma_t}{dt} &= H(t)\Sigma_t + \Sigma_t H(t) \\ &= 2I + \mathbb{E}_{\mathbf{x} \sim q_t} [\nabla_{\mathbf{x}}^2 \log p(\mathbf{x})] \Sigma_t + \Sigma_t \mathbb{E}_{\mathbf{x} \sim q_t} [\nabla_{\mathbf{x}}^2 \log p(\mathbf{x})], \end{aligned} \quad (35)$$

this is equal to the Hessian form in [Eq. \(27\)](#).

The curve $\{S_t\}_{t \geq 0}$ is the horizontal lift of the curve $\{\Sigma_t\}_{t \geq 0}$. For any point S_0 in the fiber $\pi^{-1}(\Sigma_0)$, there is a unique curve $\{S_t\}_{t \geq 0}$ such that $\pi(S_0) = \Sigma_0$ and its image under the map $\pi\{S_t\}_{t \geq 0} = \{\Sigma_t\}_{t \geq 0}$. This means the Bures-Wasserstein gradient flow can be translated into the Euclidean gradient flow and if the initial point of the Euclidean gradient flow is given, then the flow curve is unique.

Notice that the horizontal space $\mathcal{H}_S = \{X | XS^{-1} \text{ is symmetric}\}$ indicates $\forall X \in \mathcal{H}_S, XS^{-1}$ is symmetric. In another coordinate system, we can have $d\pi_S(X) = XS^{-1}$, this gives another form of Riemannian gradient,

$$\text{gradKL}(q_\theta || p) = \nabla_S \text{KL}(q_\theta || p) S^{-1}, \quad (36)$$

which is the Bures-Wasserstein gradient of the KL divergence w.r.t. the covariance matrix studied by [\(Altschuler et al., 2021; Lambert et al., 2022; Diao et al., 2023\)](#)

Remark. The Frobenius distance function $\|A - B\|_{\mathbb{F}}^2 = \text{tr}(AA^T + BB^T - 2A^T B)$ is not the intrinsic Riemannian distance by the metric tensor \mathcal{G} because the space of non-singular matrices $\mathbb{S}^{n \times n}$ is not connected, i.e., $\forall A, B \in \mathbb{S}^{n \times n}$, the straight line segment $Z(t) = tA + (1-t)B, t \in [0, 1]$ may cross the set of singular matrices. However, the space $\mathbb{S}^{n \times n}$ can be separated into two connected subspaces: the set of positive-definite matrices $\mathbb{S}_+^{n \times n}$ and the set of negative-definite matrices $\mathbb{S}_-^{n \times n}$. Each can be equipped with the Frobenius distance given by the metric tensor \mathcal{G} . If the curve $\{\Sigma_t\}_{t \geq 0}$ is smooth, its horizontal lift has to stay within the connected area, e.g., if the initialization $S_0 \in \mathbb{S}_+^{n \times n}$, the curve $\{S_t\}_{t \geq 0}$ stays within $\mathbb{S}_+^{n \times n}$. On the other hand, if we use the Monte Carlo method to evaluate gradients, there is always a small perturbation added to the matrix S_t to avoid being singular matrices. Practically, we can ignore the disconnected property of $\mathbb{S}^{n \times n}$.

D The Path-Derivative Gradient of f -Divergence

D.1 Proof of Lemma 2

Given the f -divergence as

$$\mathcal{F}_f(q) = \mathcal{D}_f(p||q) = \int f\left(\frac{p(\mathbf{x})}{q(\mathbf{x})}\right) q(\mathbf{x}) d\mathbf{x}.$$

Let $\phi \in \mathcal{P}(\mathbb{R}^n)$ be an arbitrary test function, the first variation $\frac{\delta \mathcal{F}_f}{\delta q}$ is given by

$$\begin{aligned} \int \frac{\delta \mathcal{F}_f}{\delta q}(\mathbf{x}) \phi(\mathbf{x}) d\mathbf{x} &= \lim_{\tau \rightarrow 0} \frac{\mathcal{F}_f(q + \tau \phi) - \mathcal{F}_f(q)}{\tau} \\ &= \left. \frac{d}{d\tau} \mathcal{F}_f(q + \tau \phi) \right|_{\tau=0} \\ &= \left. \frac{d}{d\tau} \int f\left(\frac{p}{q + \tau \phi}\right)(\mathbf{x}) (q(\mathbf{x}) + \tau \phi(\mathbf{x})) d\mathbf{x} \right|_{\tau=0} \\ &= \int \left\{ f\left(\frac{p}{q + \tau \phi}\right)(\mathbf{x}) \phi(\mathbf{x}) - f'\left(\frac{p}{q + \tau \phi}\right)(\mathbf{x}) \frac{p(\mathbf{x}) \phi(\mathbf{x})}{q(\mathbf{x}) + \tau \phi(\mathbf{x})} \right\} d\mathbf{x} \Big|_{\tau=0} \\ &= \int \left\{ f\left(\frac{p}{q}\right) - f'\left(\frac{p}{q}\right) \frac{p}{q} \right\}(\mathbf{x}) \phi(\mathbf{x}) d\mathbf{x}. \end{aligned}$$

Thus,

$$\frac{\delta \mathcal{F}_f}{\delta q} = f(r) - r f'(r), \quad \text{where } r = \frac{p}{q}.$$

This gives the Wasserstein gradient $\nabla_{W_2} \mathcal{F}_f(q) = \nabla_{\mathbf{x}} [f(r) - r f'(r)]$.

D.2 Proof of Proposition 3

First, we write f -divergences

$$\mathcal{D}_f(p||q_\theta) = \mathbb{E}_{\mathbf{x} \sim q_\theta} [f(r(\mathbf{x}; \theta))], \quad \text{where } r(\mathbf{x}; \theta) = \frac{p(\mathbf{x})}{q(\mathbf{x}; \theta)},$$

as

$$\begin{aligned} \mathcal{D}_f(p||q_\theta) &= \mathbb{E}_{\mathbf{x} \sim q_\theta} [r f'(r) - r f'(r) + f(r)] \\ &= \mathbb{E}_{\mathbf{x} \sim p} [f'(r(\mathbf{x}; \theta))] - \mathbb{E}_{\mathbf{x} \sim q_\theta} [r(\mathbf{x}; \theta) f'(r(\mathbf{x}; \theta)) - f(r(\mathbf{x}; \theta))]. \end{aligned} \quad (37)$$

Eq. (37) is also a result from the dual representation of f -divergences (Nguyen et al., 2010). We next apply ∇_θ to both sides of Eq. (37),

$$\nabla_\theta \mathcal{D}_f(p||q_\theta) = \nabla_\theta \mathbb{E}_{\mathbf{x} \sim p} [f'(r(\mathbf{x}; \theta))] - \nabla_\theta \mathbb{E}_{\mathbf{x} \sim q_\theta} [r(\mathbf{x}; \theta) f'(r(\mathbf{x}; \theta)) - f(r(\mathbf{x}; \theta))]. \quad (38)$$

Notice that the reparameterization is given by

$$\mathbf{x}_\theta = g(\mathbf{z}; \theta) \sim q(\mathbf{x}; \theta), \quad \mathbf{z} \sim \xi.$$

The first term of the R.H.S. of Eq. (38) can be written as

$$\begin{aligned} \nabla_\theta \mathbb{E}_{p(\mathbf{x})} [f'(r(\mathbf{x}; \theta))] &= \int p(\mathbf{x}) \nabla_\theta f'(r(\mathbf{x}; \theta)) d\mathbf{x} \\ &= \int p(\mathbf{x}) f''(r(\mathbf{x}; \theta)) \cdot \nabla_\theta r(\mathbf{x}; \theta) d\mathbf{x} \\ &= \int q(\mathbf{x}; \theta) r(\mathbf{x}; \theta) f''(r(\mathbf{x}; \theta)) \cdot \nabla_\theta r(\mathbf{x}; \theta) d\mathbf{x}, \quad \text{via the importance weight} \\ &= \int \xi(\mathbf{z}) r(\mathbf{x}_\theta; \theta) f''(r(\mathbf{x}_\theta; \theta)) \cdot \nabla_\theta r(\mathbf{x}; \theta) \Big|_{\mathbf{x}=\mathbf{x}_\theta} d\mathbf{z}, \quad \text{by LOTUS} \end{aligned}$$

(39)

The second term of the R.H.S. is

$$\begin{aligned}
& \nabla_{\theta} \mathbb{E}_{\mathbf{x} \sim q_{\theta}} [r(\mathbf{x}; \theta) f'(r(\mathbf{x}; \theta)) - f(r(\mathbf{x}; \theta))] \\
&= \nabla_{\theta} \mathbb{E}_{\mathbf{z} \sim \xi} [r(\mathbf{x}_{\theta}; \theta) f'(r(\mathbf{x}_{\theta}; \theta)) - f(r(\mathbf{x}_{\theta}; \theta))], \text{ by LOTUS} \\
&= \int \xi(\mathbf{z}) \nabla_{\theta} [r(\mathbf{x}_{\theta}; \theta) f'(r(\mathbf{x}_{\theta}; \theta)) - f(r(\mathbf{x}_{\theta}; \theta))] d\mathbf{z}, \\
&= \int \xi(\mathbf{z}) r(\mathbf{x}_{\theta}; \theta) f''(r(\mathbf{x}_{\theta}; \theta)) \cdot \nabla_{\theta} r(\mathbf{x}_{\theta}; \theta) d\mathbf{z}, \\
&= \int \xi(\mathbf{z}) r(\mathbf{x}_{\theta}; \theta) f''(r(\mathbf{x}_{\theta}; \theta)) \cdot [\nabla_{\mathbf{x}} r(\mathbf{x}_{\theta}; \theta) \circ \nabla_{\theta} \mathbf{x}_{\theta} + \nabla_{\theta} r(\mathbf{x}; \theta)|_{\mathbf{x}=\mathbf{x}_{\theta}}] d\mathbf{z}, \text{ by Eq. (28)}.
\end{aligned} \tag{40}$$

Eq. (39) - Eq. (40), we have

$$\begin{aligned}
\nabla_{\theta} \mathcal{D}_f(p||q_{\theta}) &= -\mathbb{E}_{\mathbf{z} \sim \xi} [r(\mathbf{x}_{\theta}; \theta) f''(r(\mathbf{x}_{\theta}; \theta)) \cdot \nabla_{\mathbf{x}} r(\mathbf{x}_{\theta}; \theta) \circ \nabla_{\theta} \mathbf{x}_{\theta}] \\
&= -\mathbb{E}_{\mathbf{z} \sim \xi} [h'(r(\mathbf{x}_{\theta}; \theta_s)) \cdot \nabla_{\theta} r(\mathbf{x}_{\theta}; \theta_s)], \text{ by Eq. (29)} \\
&= -\mathbb{E}_{\mathbf{z} \sim \xi} [\nabla_{\theta} h(r(\mathbf{x}_{\theta}; \theta_s))],
\end{aligned} \tag{41}$$

where $h(r) = r f'(r) - f(r)$.

We summarize some typical f -divergences and their associated h functions in [Table 1](#). It can be seen that for all α -divergences where $h'(r) = r^{\alpha-1}$, if the target $p(\mathbf{x})$ is unnormalized, we have

$$h' \left(\frac{p(\mathbf{x})}{q(\mathbf{x})} \right) \propto h' \left(\frac{p_{\text{true}}(\mathbf{x})}{q(\mathbf{x})} \right), \tag{42}$$

where $p_{\text{true}}(\mathbf{x}) = p(\mathbf{x}) / \int p(\mathbf{x}) d\mathbf{x}$. Hence, according to Eq. (41), the normalizing constant only affects the scales of the path-derivative gradient, which can be folded into the learning rate.

Table 1: f -divergences and associated h functions.

	$f(r)$	$h(r) = r f'(r) - f(r)$	$h'(r)$
Reverse KL ($\alpha = 0$)	$-\log r$	$\log r - 1$	$\frac{1}{r}$
Forward KL ($\alpha = 1$)	$r \log r$	r	$\frac{1}{r}$
χ^2 ($\alpha = 2$)	$(r - 1)^2$	$r^2 - 1$	$2r$
Hellinger ($\alpha = 0.5$)	$(\sqrt{r} - 1)^2$	$\sqrt{r} - 1$	$\frac{1}{2\sqrt{r}}$
α -divergence ($\alpha \neq 0, 1$)	$\frac{r^{\alpha} - \alpha r - (1 - \alpha)}{\alpha(\alpha - 1)}$	$\frac{r^{\alpha} - 1}{\alpha}$	$r^{\alpha - 1}$

E Experiments

Codes are available on <https://github.com/YiMX/Bridging-the-gap-between-VI-and-WGF>.

E.1 The Illustrative Example on Gaussians

In Section 3.3, the target distribution $p(\mathbf{x})$ is a Gaussian $\mathcal{N}(\mu, \Sigma)$ with $\mu = (0.0, 0.0)$ and $\Sigma = ((0.8, 0.4), (0.4, 0.8))$. The initial variational distribution is Gaussian with $\mu = (4.0, 2.0)$ and identity covariance matrix I . In Figure 1, we use 5 particles to evaluate the Monte Carlo gradients for each algorithm and the learning rate is set to be 0.01. In Figure 4, the sample size of the Monte Carlo gradient increases to 100, we can observe that the variance of BBVI-rep becomes smaller and all three algorithms still generate the same visible evolution. The target density in the right figure in Figure 4 follows the Rosenbrock density function,

$$p(\mathbf{x}) \propto \exp \{-a(\mathbf{x}_1 - \mu)^2 - b(\mathbf{x}_2 - \mathbf{x}_1^2)^2\}, \quad \mathbf{x} = (\mathbf{x}_1, \mathbf{x}_2), \quad (43)$$

where $a = 1.0, b = 1.0, \mu = 1.0$.

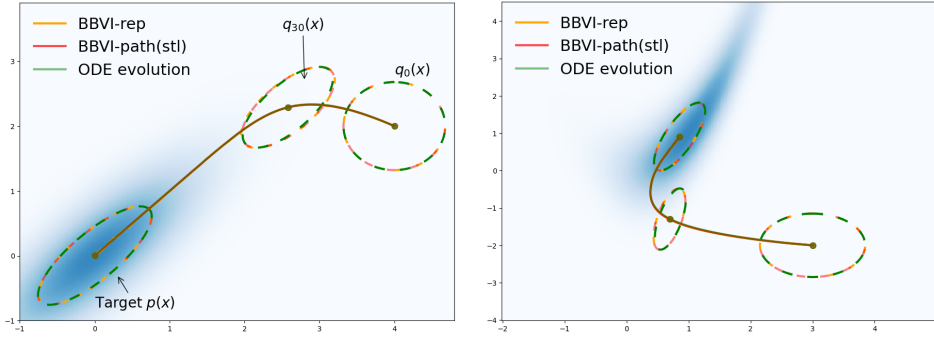


Figure 4: Mean and covariance evolution of Gaussians. The sample size for the Monte Carlo gradient is 100.

E.2 On The Path-Derivative Gradient of f -Divergences

The path-derivative gradient of f -divergences is given by

$$\nabla_{\theta} \mathcal{D}_f(p||q_{\theta}) = -\mathbb{E}_{\mathbf{z} \sim \xi} [\nabla_{\theta} h(r(\mathbf{x}_{\theta}; \theta_s))], \quad (44)$$

which defines a surrogate Monte Carlo objective

$$L(\theta) = -\mathbb{E}_{\mathbf{z} \sim \xi} [h(r(\mathbf{x}_{\theta}; \theta_s))].$$

To this end, we can evaluate this surrogate Monte Carlo objective and differentiate it to get the unbiased gradient estimator of an f -divergence such that we can perform BBVI, as shown in Algorithm 2.

Algorithm 2 BBVI with the path-derivative gradient of f -divergence

Require: unnormalized density $p(\mathbf{x})$, variational family $q(\mathbf{x}; \theta)$, the associated $h(r) = r f'(r) - f(r)$ and learning rate τ .

while not converged **do**

1. Sample N particles $\{\mathbf{z}^i\}_{i=1 \dots N} \sim \xi$ and reparameterizing $\mathbf{x}_{\theta}^i = g(\mathbf{z}^i; \theta)$.
2. Compute $r(\mathbf{x}_{\theta}^i; \theta_s) = p(\mathbf{x}_{\theta}^i)/q(\mathbf{x}_{\theta}^i; \theta_s)$, where stop gradient operator is applied to θ .
3. Compute $L(\theta) = -\frac{1}{N} \sum_i h(r(\mathbf{x}_{\theta}^i; \theta_s))$.
4. $\theta \leftarrow \theta - \tau \nabla_{\theta} L(\theta)$ via back-propagation.

end while

E.2.1 Toy Example

In this section, we illustrate [Algorithm 2](#) using different f -divergences. The target distribution is an unnormalized 2D Gaussian $\mathcal{N}(\mu, \Sigma)$ with $\mu = (0.0, 0.0)$ and $\Sigma = ((0.5, 0.3), (0.3, 0.5))$ and the variational distribution is also a 2D Gaussian initialized at $\mu = (1.0, 0.5)$ and $\Sigma = ((1.0, 0.0), (0.0, 1.0))$. We plot the trajectories of the means of Gaussian variational distributions in [Figure 5](#). For comparison, we also plot the trajectories obtained via BBVI using the reparameterization gradient (BBVI-rep). To allow for computing the reparameterization gradient, we borrow the ground truth normalized target distribution’s density. In [Figure 5](#), we can observe that different f -divergences produce different trajectories of Gaussian means in Euclidean space, this corresponds to distilling different gradient flows (curves of marginal probabilities) in Wasserstein space. We also observe that the trajectories of BBVI-path exactly evolve to the target mean under all f -divergences, whereas the trajectories of BBVI-rep fluctuate around the target mean under reverse KL divergence and forward KL divergence. This phenomenon corresponds to [Eq. \(??\)](#) where the variance of the path-derivative gradient diminishes if the variational distribution well approximates the target distribution such that the Wasserstein gradient becomes zero, also known as "sticking the landing" ([Roeder et al., 2017](#)). This fluctuation of BBVI-rep does not happen under χ^2 divergence and Hellinger divergence.

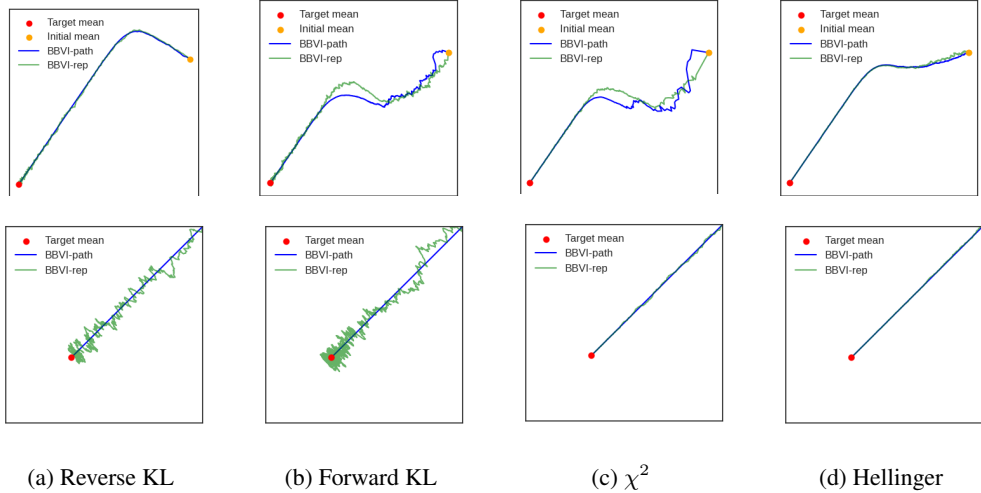


Figure 5: Trajectories of means of Gaussian variational distributions. The bottom figures are the plots zoomed in around the target mean.

E.3 Bayesian Logistic Regression

In this part, we implement the path-derivative gradient for Bayesian logistic regression using UCI dataset [Asuncion and Newman \(2007\)](#). For comparison, the baseline is the standard VI method—reverse KL with reparameterization trick and "CHIVI" method ([Dieng et al., 2017](#)). Note that the reparameterization gradient is intractable due to the normalizing constant, except for the reverse KL. The variational family is diagonal Gaussian. In this experiment, we use the same trick as [Dieng et al. \(2017\)](#) to adjust the density ratio per iteration in [Algorithm 2](#) to enhance the numerical stability,

$$r(\mathbf{x}_\theta^i; \theta_s) = \exp \left[\log r(\mathbf{x}_\theta^i; \theta_s) - \max_i \log r(\mathbf{x}_\theta^i; \theta_s) \right], \quad (45)$$

since the constant $\max_i \log r(\mathbf{x}_\theta^i; \theta_s)$ only affects the scale of the path-derivative gradient according to [Eq. \(42\)](#).

Below is the test set accuracy with standard deviation, calculated with 32 posterior samples. In [Table 2](#), we found VI with the path-derivative gradient generalizes well to different datasets compared to the standard VI method and CHIVI.

Table 2: Test accuracy. Higher is better.

Dataset	RKL (rep)	CHIVI	RKL (path)	FKL (path)	χ^2 (path)	Hellinger (path)
Heart	0.871 \pm 0.017	0.786 \pm 0.080	0.872 \pm 0.024	0.815 \pm 0.069	0.792 \pm 0.066	0.828 \pm 0.055
Ionos	0.783 \pm 0.022	0.670 \pm 0.094	0.782 \pm 0.022	0.665 \pm 0.090	0.664 \pm 0.094	0.664 \pm 0.103
Wine	0.720 \pm 0.015	0.694 \pm 0.041	0.720 \pm 0.015	0.693 \pm 0.046	0.692 \pm 0.047	0.703 \pm 0.035
Pima	0.775 \pm 0.016	0.731 \pm 0.037	0.776 \pm 0.013	0.726 \pm 0.035	0.733 \pm 0.037	0.748 \pm 0.029

E.4 Extension to Gaussian Mixture Models

In this section, we discuss how to apply the path-derivative gradient to update the parameters of Gaussian mixture variational families. Using Gaussian mixture models (GMMs) enriches the flexibility of the approximation. A GMM comprises K individual Gaussian distributions, we denote m_k as the weight and θ_k as the parameter for the k -th Gaussian component. The probability density function of GMM is

$$q(\mathbf{x}; \theta, m) = \sum_{k=1}^K m_k q_k(\mathbf{x}; \theta_k), \quad \sum_{k=1}^K m_k = 1. \quad (46)$$

The reparameterization path of the sample $\mathbf{x}_{\theta, m} \sim q(\mathbf{x}; \theta, m)$ from GMMs is not directly differentiable since it requires discrete sampling from a categorical distribution to determine in which component the sample is generated. We should notice the surrogate Monte Carlo objective $L(\theta, m)$ for GMMs can be decomposed via conditional sampling as

$$L(\theta, m) = -\mathbb{E}_{\mathbf{x} \sim q(\mathbf{x}; \theta, m)} [h(r(\mathbf{x}; \theta_s, m_s))] = -\sum_{k=1}^K m_k \mathbb{E}_{\mathbf{z} \sim \xi} [h(r(\mathbf{x}_{\theta_k}; \theta_s, m_s))], \quad (47)$$

where $\mathbf{x}_{\theta_k} = g(\mathbf{z}; \theta_k)$ is sampled from the k -th component distribution $q_k(\mathbf{x}; \theta_k)$. With the help of the stop gradient operator, the surrogate Monte Carlo objective disentangles the interaction of the parameters of GMMs such that the gradients for each θ_k and m_k depend only on samples from the k -th component. We give a summary of the distilled Wasserstein gradient flows with GMM variational families in [Algorithm 3](#).

Algorithm 3 Variational Inference with Gaussian Mixture Variational Families

Require: unnormalized density $p(\mathbf{x})$, variational distribution $q(\mathbf{x}; \theta, m) = \sum_{k=1}^K m_k q_k(\mathbf{x}; \theta_k)$, the associated function $h(r) = r f'(r) - f(r)$ and learning rate τ .

while not converge **do**

for $k = 1 \dots K$ **do**

1. Sample N particles $\{\mathbf{z}^i\}_{i=1 \dots N} \sim \xi$ and reparameterizing $\mathbf{x}_{\theta_k}^i = g(\mathbf{z}^i; \theta_k)$.
2. Compute $r_i = p(\mathbf{x}_{\theta_k}^i) / q(\mathbf{x}_{\theta_k}^i; \theta_s, m_s)$, where the stop gradient operator is applied.
3. Compute $\ell_k = \frac{1}{N} \sum_i h(r_i)$.

end for

4. Compute $L(\theta, m) = -\sum_{k=1}^K m_k \ell_k$.

5. $(\theta, m) \leftarrow (\theta, m) - \tau \nabla_{(\theta, m)} L(\theta, m)$ and via back-propagation.

end while

We show how [Algorithm 3](#) performs on approximating Rosenbrock density in Eq. (43) (banana distributions). The number of components is set to 5 and we add Softmax activations to ensure the sum of weights is equal to 1, the approximated variational GMMs are shown in [Figure 3](#) with contour plots of their density functions.

E.4.1 Approximating 1D Gaussian Mixture Distributions

The target distribution is a 3-mode Gaussian mixture distribution with density function with a normalizing constant,

$$p(\mathbf{x}) \propto 0.4\mathcal{N}(-1.0, 0.25) + 0.3\mathcal{N}(0.8, 0.25) + 0.3\mathcal{N}(3.0, 0.64).$$

The variational distribution has the density function,

$$q(\mathbf{x}; \theta, m) = \sum_{k=1}^K m_k q_k(\mathbf{x}; \theta_k), \quad \sum_{k=1}^K m_k = 1,$$

where each $q_k(\mathbf{x}; \theta_k)$ is a Gaussian distribution. We implement [Algorithm 3](#) to approximate this target under f -divergences via Gaussian mixture variational families that have different numbers of components K . The density plots of the target distribution and variational distributions are reported in [Figure 6](#). We can observe that with K increases, the resulting approximations are more accurate.

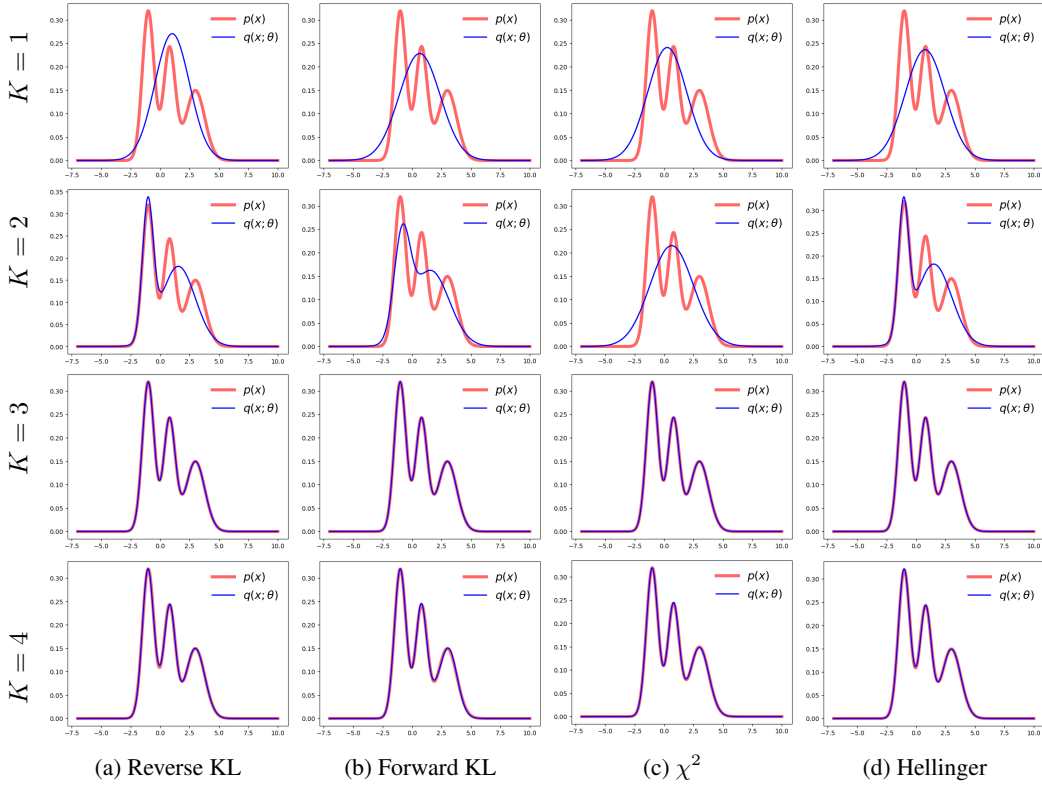


Figure 6: Approximating a target Gaussian mixture distribution via variational GMMs with different numbers of components.